July 12th, 2020

Dr. Craig Scratchley
School of Engineering Science
Simon Fraser University
Burnaby, BC, V5A 1S6

Re: ENSC 405W/ENSC 440 Design Specification for VALIS

Dear Dr. Scratchley,

The attached document outlines the design specifications for VALIS, a Vascular Acoustic Light Imaging System. VALIS is a photoacoustic imaging system specialized for imaging vasculature. Our goal is to design a photoacoustic imaging system that is available for smaller scale research labs, by reducing both cost and size of the system compared to current similar products on the market. Furthermore, we aim to improve the versatility of imaging by implementing a handheld device to receive the acoustic signals, giving more freedom for real time imaging.

Detailed Information for the design of VALIS can be found in the enclosed document. The design specifications include details on the light source and optics, transducer, data acquisition unit, image processing and reconstruction, as well as any relevant safety considerations. The document outlines each major component of the overall system and gives an overview of how they combine to create the system as a whole.

Our capable team consists of 6 talented SFU senior engineering students; Ryan Chahal, Glenn Ferguson, John Kim, Alex McGovern, Steven McLeod, and Sean Paulsen. We come from various backgrounds, with experience in optics, electronics, software, and other forms of hardware, which we will combine to make an outstanding affordable photoacoustic imaging system.

Thank you for taking the time to review our design specifications document. If you have any questions or inquiries, please feel free to reach out to us through our GitLab or contact our Chief Communications Officer, Glenn Ferguson, at gferguso@sfu.ca.

Sincerely,

Sean Paulsen
Chief Executive Officer
VivoLux

Enclosed: Design Specifications for VALIS

PoC Prototype Design Specifications
for
VALIS
Imaging the Sound of Light

Team Members	Sean Paulsen	spaulsen@sfu.ca	CEO
	Glenn Ferguson	gferguso@sfu.ca	CCO
	John Kim	jka157@sfu.ca	CIO
	Ryan Chahal	rschahal@sfu.ca	COO
	Alex McGovern	amcgover@sfu.ca	CSO
	Steven McLeod	samcleod@sfu.ca	CTO

Submitted To

Dr. Craig Scratchley — ENSC 405W
Dr. Andrew Rawicz — ENSC 440
School of Engineering Science
SFU

Contact Person

Glenn Ferguson
gferguso@sfu.ca
778-235-1184

Issue Date July 12th, 2020

Version 1.0

Abstract

There are numerous different imaging modalities ranging from ionizing methods such as x-rays to techniques involving powerful magnetic fields like MRIs. However, there are drawbacks to many of these modern imaging techniques, including but not limited to exposure to harmful radiation, cost, reduced image quality, and availability. Photoacoustic imaging is a safe versatile high-quality imaging modality.

VivoLux aims to provide an affordable photoacoustic imaging system, specialized for imaging vasculature. VALIS will be a compact system with the transducer and light source mounted on a handheld device, providing versatility in real time imaging. This allows users to image various areas of the subject or patient in a single imaging session. This document will outline the design specifications required for VALIS to be affordable and have real time imaging versatility. VALIS will bring photoacoustic imaging to the untouched market of researchers looking for a high quality affordable vascular imaging system.

This document provides a detailed overview of the required specifications for VALIS, a photoacoustic imaging system. The system consists of four major components:

1. The light source and optics for illuminating the region being imaged.

2. The transducer for detecting any acoustic waves generated from the illuminated tissue after absorbing light produced by the Light source and optical system.

3. The data acquisition unit for acquiring the data, performing any necessary preprocessing, and controlling the flow of data from the transducer to the image processing and reconstruction component.

4. The software for converting the raw data from the transducer into usable images.

Table of Contents

List of Figures

List of Tables

Equations

Glossary

Term	Description
AAMI - Association for the Advancement of Medical Instrumentation	AAMI is a non-profit organization dedicated to the development, management, and use of safe and effective health technology.
ADC - Analog-to-Digital Converter	A system that converts an acquired analog signal to a digital signal for processing by a computer.
BP - Backprojection	A common image reconstruction method which recurring landmarks are repositioned to form an image.
CS - Computed Sensing	An iterative method of reconstructing images which calculates the error of an image and corrects it.
CSA - Canadian Standards Association	A Canadian organization dedicated to developing, maintaining, and certifying industry standards.
CT - Computed Tomography	A medical scan that uses computer processed combinations of x-rays taken at different angles to develop images of an object's interior.
DAC - Digital-to-Analog Converter	A system that converts a digital signal, from a computer, and outputs an analog signal.
DAQ - Data Acquisition	The process of sampling measured signals of physical conditions and converting them to digital signals for processing.
EM - Electromagnetic	Describes electrical and magnetic forces and effects produced by an electric current.
FBP - Filtered Backprojection	Image reconstruction methodology utilizing the Inverse Radon Transform
GUI - Graphical User Interface	Form of user interface that allows users to interact with electronic devices through graphical icons
IEEE - Institute of Electrical and Electronics Engineers	The Institute of Electrical and Electronics Engineers is a professional association for electronic engineering and electrical engineering
IEC - International Electrotechnical Commission	An organization that prepares and publishes standards pertaining to electrical, electronics and any related technologies.

IR - Infrared	Light whose wavelength is outside the visible spectrum for a human and is longer than red light and shorter than microwaves (approximately 700 nm to 1 mm).
ISO - International Standards Organization	A standard setting organization composed of representatives from various national standards organizations.
LED - Light Emitting Diode	A semiconducting light source that emits light when current flows through it.
MPE - Maximum Permissible Exposure	The highest laser power that is considered safe for the eye or skin.
MRI - Magnetic Resonance Imaging	Form of medical imaging using a strong magnetic field and high frequency radio waves.
NIR - Near Infrared	Short wavelength infrared light (approximately 700 nm to 3000 nm)
PA - Photoacoustic	Acoustic wave generation due to light absorption.
PAI - Photoacoustic Imaging	Imaging modality that generates images using the photoacoustic effect
PACT - Photoacoustic Computed Tomography	A specialized form of photoacoustic imaging.
PAT - Photoacoustic Tomography	A specialized subset of photoacoustic imaging.
PLA - Polyactic acid	Widely used filament for 3D printing
PZT - Lead Zirconate Titanate	A piezoelectric ceramic material commonly used in ultrasonic transducers.
ROI - Region of Interest	Bounded area undergoing analysis.

1. Introduction

1.1 Background

There is a wide range of macroscopic imaging techniques for both clinical and research purposes. Advances in imaging systems and techniques have offered a wealth of knowledge on various types of biological tissue. X-rays, high-frequency forms of electromagnetic (EM) radiation, can image dense tissue such as the bones. Dense tissue readily absorbs x-rays, whereas through soft tissue does not. This results in creating a high contrast image. Computed tomography (CT) scans are a more sophisticated type of x-ray machines that use several x-ray beams to recreate a more complex and accurate reconstruction of the imaged tissue [1].

In contrast to x-rays and CT scans, magnetic resonance imaging (MRI) is an imaging modality that can image soft tissue. MRIs use a strong magnetic field to orient water molecules in the same direction. Protons in the water molecules become aligned, changing the proton's spin. A radiofrequency is then passed through the patient, perturbing the alignment of the protons. When the radiofrequency is turned off, the protons realign with the magnetic field and emit a form of energy in the process [2]. This energy can be measured and used to recreate an image. Typically, a contrast dye is injected into the patient before image acquisition to improve image clarity.

Another soft tissue imaging modality is ultrasound, also known as sonography. Ultrasound imaging generates high-frequency acoustic waves from typically piezoelectric transducers via electrical stimulation. A portion of the acoustic waves will reflect off the tissue, while the rest will pass through. The same piezoelectric transducer can receive the incoming acoustic waves and transform them into electrical signals. Based on the intensity and timing of the received signal, an image can be reconstructed. This can generate images safely and in real-time. Additionally, doppler ultrasounds can measure blood flow in vivo.

Although these forms of medical imaging have proven useful and are widely used in modern medical practices, there are several risks and limitations associated with them. X-rays are a form of ionizing radiation, which upon exposure is harmful. Ionizing rays have the potential to alter atoms they interact with, leading to changes in the genetic structure and material found within cells. This can cause harm to anyone exposed to ionizing radiation and increases the risk of cells becoming carcinogenic. MRIs avoid the problem of ionizing radiation; however, they are expensive to purchase and operate. This is a limiting factor to their availability and often leads to long waitlists for MRI usage. Moreover, due to the strong magnetic fields involved in MRIs, complications may arise for any patients with metal implants. Furthermore, neither MRI nor x-ray imaging methods can be done in real-time. Ultrasounds are a non-ionizing imaging modality, however, there are limitations in image resolution and quality with ultrasounds. Acoustic waves do not travel well through dense tissue or gaseous mediums such as bone or air in the lungs [3].

Purely optical imaging is another imaging technique. A light source in the visible or near-infrared (NIR) spectrum is used to illuminate tissue. When passing through turbid mediums, photon scattering and absorption occurs, which can be measured using optical cameras

external to the medium being imaged. This is considered a safe non-invasive imaging modality; however, it is heavily limited due to photon scattering. The ballistic photons, photons that do not experience path deviations due to scattering events, and quasi-ballistic photons, photons that experience minimal trajectory deviation, can provide structural and functional information about the tissue. In contrast, scattered light typically acts as noise. When traveling through turbid media, it is highly likely that the light will be scattered, changing the trajectory of the protons. Since the probability of scattering events increases with the thickness of the imaged medium, purely optical imaging is only practical for superficial tissue [4].

Photoacoustic imaging (PAI) is a safe, non-invasive, imaging modality that can produce high-resolution images. PAI can offer higher spatial resolution compared to sonography since optical scattering is not a limiting factor for the spatial resolution and the acoustic waves travel half the distance in PAI [5]. This means the acoustic attenuation is half that of traditional ultrasound at the same frequency. Also, imaging can be done in real-time. PAI can provide high-quality imaging without many of the caveats of other imaging modalities. Unfortunately, current PAI systems are quite costly. VivoLUX aims to design an affordable PAI system capable of imaging microvasculature.

1.2 Photoacoustic Imaging

Chromophores are the part of a molecule that is capable of absorbing photons. PAI uses the optical absorption characteristics of chromophores to provide energy to certain types of tissue. Upon illumination, the tissue whose peak absorption wavelength corresponds to the wavelength of the excitation source, absorbs the incoming photons. Upon absorption, the molecule enters an excited state. Typically, the excited molecular state is unstable and short-lived. Consequently, the energy is rapidly dissipated either through radiant methods or to neighbouring molecules. In PAI, the illuminated tissue dissipates a large amount of the energy as heat.

Through rapid heating, though only by a fraction of a degree [6], thermal expansion and pressure build-up occurs at the illuminated area. As a result, acoustic waves are generated and propagate through the neighbouring tissue. The amplitude of the acoustic signals is linearly proportional to the intensity of the excitation light [5]. After propagating through tissue, the acoustic waves can be measured outside of the imaging medium. Using the measured signal amplitudes, an image of the tissue can be constructed.

1.3 Scope

The purpose of this document is to outline in detail the technical and design specifications for VALIS, a vascular acoustic light imaging system. The specifications will describe the various design decisions with supporting reasons and evidence. The entire system will be analyzed, followed by each major component in further detail. The major components will be divided into four categories: light source, transducer, data acquisition, and image processing and reconstruction. For each major component, the design decisions will be justified in their respective sections.

An appendix is provided to outline a testing plan for the proof of concept as well as providing further details regarding the user interface, appearance, and relevant engineering standards for both the proof of concept and prototype.

1.4 Design Classification

The design classification will adhere to the following format throughout this document:

Des. (Section #).(Subsection #).(Requirement #)-(Stage of Development)

The stages of development are as follows:

Designation	Stage of Development
C	Proof of Concept
P	Prototype
F	Final Product

Table 1.4.1 Development stages and abbreviations

The “Proof of Concept” stage denotes the requirements that will be implemented by the end of ENSC 405W, while the “Prototype” requirements must be met by the end of ENSC 440. The “Final Product” requirements outline the standards to which the production unit must conform.

2. System Overview

The system consists of four major components: the light emitting diode (LED) light source, the transducer, the data acquisition unit, and the image processing and reconstruction unit. Detailed specifications will be provided for each component in their respective sections. Figure 2.0.1a shows the entire system, while figure 2.1b is a simplified block diagram of the system.

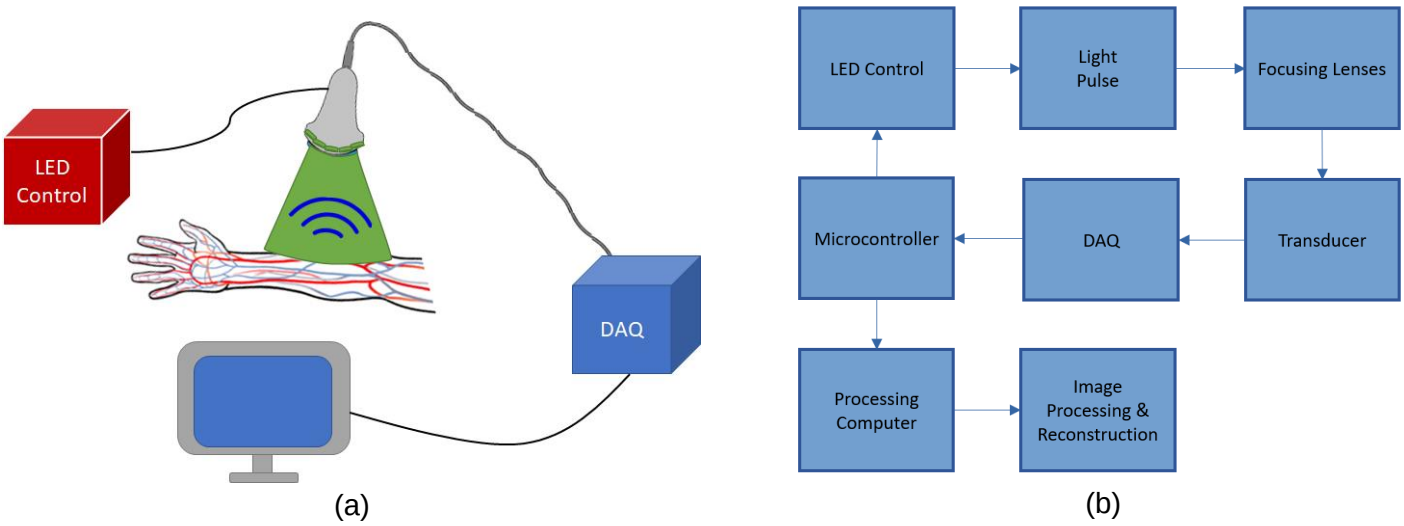

Figure 2.0.1: (a) An overview of the main components of the Photoacoustic Imaging System, including the light source, LED controller, ultrasound transducer, DAQ unit and computer for processing. (b) Simplified block diagram of the main components of the system

The system as a whole functions by first illuminating the imaging area with the light source. The light source for VALIS will consist of 10 high power LEDs each utilizing a focusing lens to restrict the illuminated area. After the tissue has absorbed the photons and generated the acoustic waves, the transducer will measure and record the incoming acoustic waves from outside the medium being imaged. This makes the device completely non-invasive as well as non-ionizing. The transducer will be situated on the end of a handheld device. The light source, lenses, transducer, and heat sink will all be integrated into a single handheld probe coupled to a communication and power line. This communication cable will be connected to a data acquisition/control module which will control both the LEDs and transducer as well as acquire the raw data from the transducer which will be sent to the PC running a customized MATLAB script for processing. Our image reconstruction software will give the user an easy and intuitive method of analyzing the tissue of interest.

Many of the components for VALIS will be standard parts that are readily available for purchase. Therefore, they will retain the ability to be repurposed rather than discarded. This will contribute to the sustainability of the final product and will decrease the amount of waste produced at the end of its useful life.

Table 2.0.1 shown below outlines all the requirements of the whole system.

Design ID	Design Specification
Des. 2.0.1-C	Illuminate biological tissue at a frequency that emphasizes absorption by hemoglobin
Des. 2.0.2-C	Generate acoustic waves upon illumination on hemoglobin
Des. 2.0.3-C	Detect acoustic waves and record signal changes measured by the sensor corresponding to light source pulses
Des. 2.0.4-P	Produce an image in 2-Dimensions of patients or phantoms vasculature in real-time
Des. 2.0.5-P	Product will be ergonomic and safe for use
Des. 2.0.6-P	Operation will be intuitive and user friendly
Des. 2.0.7-P	Total unit cost will be less than $1500 CAD to build

Table 2.0.1 General system requirements

3. Component Requirements

This section will define what is required for our system. The major components of our system are broken down into the subsections below along with their specific requirements.

3.1 Light Source and Optics

The molecular excitation source of a PAI system is a high energy, short-pulsed group of photons. Commonly, Q-switched lasers are used as a photoacoustic excitation source. However, an array of LEDs can offer an affordable, compact, and highly efficient alternative. Furthermore, overdriving LEDs at low duty cycles can offer pulses with power far exceeding their standard power ratings. To generate the excitation beam, we will use several high luminous efficacy 10W LEDs positioned around the receiving transducer. Lenses will be mounted to the LEDs in order to restrict the light to a viewing angle of ten degrees. This will focus the photons solely on the area being imaged.

Traditionally, these tunable, Q-switched, Nd:YAG lasers that are utilized in most PAI systems are extremely costly. With VALIS, our light source will not require tunability. By removing the need for tunability that is employed by my most current devices [7], we can move away from the high cost of solid-state lasers and achieve similar results. The need for tunability of a PAI system roots from manufacturers who want to develop hospital grade devices that can be used to image a range of tissue types. This approach has so far been beneficial, but this is strongly due to the lack of competitors in the market. By looking directly at some of the most promising uses for PAI systems we have selected a tissue of interest and therefore removed this need for tunability completely.

As an imaging modality that aims to identify vascular structure in-vivo, we can select a fixed wavelength of interest that corresponds to the absorption peaks of hemoglobin and deoxyhemoglobin. Figure 3.1.1. shows the absorption coefficients of abundant molecules of interest when performing PAI. At wavelengths in the visual spectrum, absorption is dominated by the oxyhemoglobin (in red) and reduced hemoglobin (in blue) except for the Melanin (in black). However, melanin is highly concentrated in small regions such as the skin [8] and rarely interferes with PAI systems. Since hemoglobin has at least an order of magnitude greater in terms of absorption at the wavelengths when compared to other relevant molecules, we have chosen to select a light source with the wavelength in the visible region, and more specifically LEDs that output at 523 nm. Figure 3.1.1 also shows a number of other abundant tissue types, and their absorption spectrum. For example, Lipids and water are both shown in brown and black, respectively. Their lower absorption coefficient, as shown in a log scale suggests that at the selected 523 nm wavelength, there will be some photon absorption. This absorption however will be magnitudes lower in both cases from that of both hemoglobin and deoxyhemoglobin which will generate lower energy acoustic waves. The result will be a high contrast image with regions of vasculature being high intensity, regions of high lipid concentration being mid intensity and regions where water molecules are most abundant the lowest intensity.

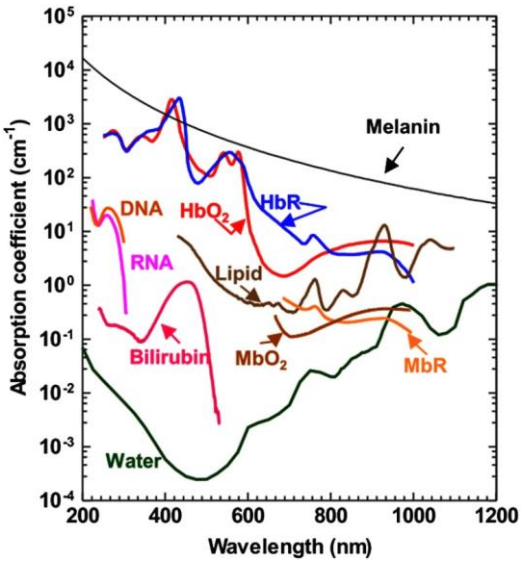

Figure 3.1.1: Absorption coefficients of chromophores of interest relative to excitation wavelength [9]

For a photoacoustic effect to occur, the pulse EM pulse must meet the thermal and stress confinement conditions. The pulse duration of the excitation source must be shorter than the time required for heat dissipation, which can be represented using the inequality shown below:

$$\tau < \tau_{th}$$

Equation 1. Thermal confinement condition [4]

In this equation, τ represents the EM pulse length, while τ_{th} represents the thermal confinement threshold. The threshold for the thermal confinement is proportional to the spatial resolution that can be obtained using the generated acoustic waves as seen in the following equation:

$$\tau_{th} = \frac{d_c^2}{4D_t}$$

Equation 2. Time for thermal expansion [4]

For the above equation, d_c is known as the characteristic linear dimension, which is directly related to the possible spatial resolution of the image. The thermal diffusivity is represented by D_t and for most soft tissue has a value of 0.14 $\frac{mm^2}{s}$ [4].

Similar to the thermal confinement condition, the pulse length is dictated by τ_s, the time for stress to traverse the heated region as seen in the following inequality:

$$\tau < \tau_s$$

Equation 3. Stress confinement condition [4]

When the absorbing tissue is heated faster than thermal expansion can occur, a localized pressure rise occurs. Faster heating results in greater pressure build ups, allowing for higher amplitude acoustic wave generation. This relation indicates the amplitude of the

acoustic waves is proportional to the power of the illumination source. Additionally, sufficient pressure build with inconsequential volume expansion is the determining factor for the stress confinement condition. The time for stress to pass through the region being heated is related to the characteristic linear dimension and the speed of sound as shown in the equation below.

$$\tau_s = \frac{d_c}{c}$$

Equation 4. Time for stress to propagate through heated region [4]

For both confinement conditions, we want to minimize d_c to maximize the spatial resolution obtainable by the acoustic waves. For the thermal confinement condition, the thermal diffusivity is a constant, whose value is dependent on the medium being imaged. In the case of the stress confinement condition, the speed of sound through the imaging medium is a constant. Therefore, the only variable parameter that can be optimized to minimize the characteristic linear dimension is the illumination source pulse duration. However, to produce a measurable photoacoustic effect, a suitable energy level must be provided for each pulse. A higher energy EM pulse corresponds to a higher amplitude acoustic wave being produced. Meanwhile, a shorter pulse duration results in higher spatial resolution. An ideal PAI system has maximal power provided per pulse with the shortest possible pulse duration. Accordingly, we are using the highest power light source possible that falls within our budget.

For each pulse, an energy level between 1 and 20 mJ is desired to have a comparable image penetration depth and SNR to that of a conventional solid-state Nd:YAG PAI system [10]. Aside from pulse power and duration, the pulse repetition rate (frequency) can improve the clarity and resolution of the acquired image. At pulse frequency ranges of 1 kHz to 10 kHz, multiple samples can be averaged while still holding a real-time output and increasing SNR. Having a frequency of 10 kHz corresponds to a period of 100 µs and therefore a pulse duration of 50 µs with a 50% duty cycle. However, if the LEDs are being overdriven, lower duty cycles may be required. We shall evaluate the benefits of lower power pulses at higher frequencies and duty cycles compared to overdriving the LEDs to acquire higher powered pulses at lower duty cycles and frequencies. Whichever method provides the best quality images will be selected. While LEDs can achieve high duty cycles, an advantage of reducing the duty cycle is to decrease the overall temperature build-up of the optics.

To shape the excitation beam produced by the high intensity LEDs we will employ a conical lens fitted on top of each LED. An image of a LED and lens are shown in figure 3.1.2. The lens is responsible for concentrating the LEDs power onto only the region of interest. Due to the LEDs and therefore the lenses placement in a row along the long axis of the transducer, the Lenses will be placed at 10-degree angle with the low side of the mounted LED closest to the transducer. A cross section of this design can be seen in figure 3.1.2c. As we have selected a lens with a 10-degree viewing angle, this will concentrate the LEDs power in the smallest possible region while still illuminating the desired tissue region. Each LED lens has a diameter of 14.5 mm. This will give a row of 5, with a 0.5 mm spacing a total length of 75 mm. Placing each LED 10 mm away from the tissue will therefore leave a total illumination area of 77 mm by 17 mm. This gives an illumination area from the combined 10 LEDs of 2618 mm^2.

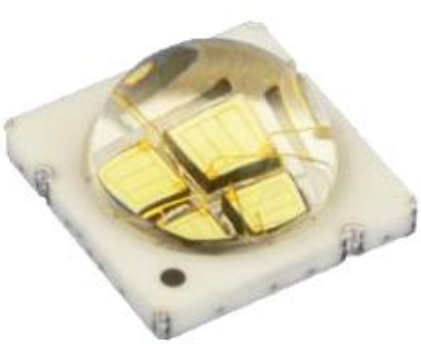

(a)

(b)

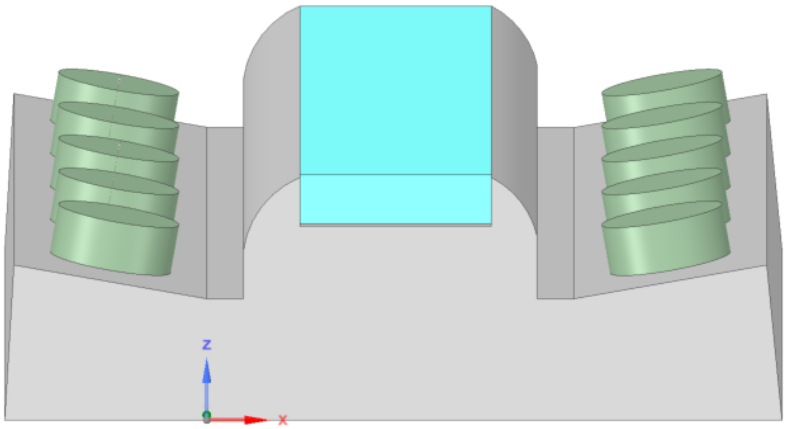

(c)

Figure 3.1.2: (a) LED Engin LZ4-00G108-0000, high power, 523 nm LED [11] (b) DBM Optix O-005s LED conical focusing lens [12] (c) Cross sectional view of LED, optical lens mounted to handheld probe showing the LED angles relative to the transducer

The design specifications for the light source and optics are indicated in table 3.1.1.

Design ID	Design Specification
Des. 3.1.1-C	An LED with a wavelength of 523 nm will be used to ensure maximum absorption by the desired tissue type.
Des. 3.1.2-C	The LED will provide an energy output between 1 and 20 mJ
Des. 3.1.3-C	The LED will be powered at a frequency between 1 kHz and 10 kHz
Des. 3.1.4-C	The LED will have a pulse duration between 10 µs and 100 ns
Des. 3.1.5-C	The LEDs illumination beam will be optically directed using a lens to focus the beam on only the region of interest
Des. 3.1.6-C	The optical fluence shall be below the MPE ratings for 523 nm light source

Table 3.1.1 Design requirements for light source and optics

3.2 Transducer

After the subject has been excited with the light source, the photoacoustic signal emitted from the thermal expansion needs to be acquired by a transducer. The time-varying detected ultrasonic signals can be spatially resolved and back-projected to reconstruct a three-dimensional image [8]. There are a variety of transducer types and geometries for acquiring the resulting photoacoustic signal. Traditionally, lead zirconate titanate (PZT) transducers, a piezoelectric ceramic material, are used for medical ultrasound. However, there are several alternatives to classical piezoelectric ceramic materials, such as capacitive transducers and purely optical methods.

Despite improvements in microfabrication techniques, PZT transducers are considered superior to their capacitive alternative, particularly for high frequency applications [11]. On the other hand, optical acoustic wave detection does not have the same frequency limitations. Optical ultrasound detection uses a laser reflecting off a transducing surface. As the ultrasonic pressure waves propagate through the imaging medium, the reflective transducing surface will experience periodic perturbations corresponding to the frequency of the acoustic waves. The reflected beam will carry information on the displacements at the reflective surface, which can be decoded and measured using interferometry [11]. The measured signal is dependent entirely on the amplitude of the optical phase shift which leads to one caveat of this optical method; the measured signal is often weak. Therefore, etalons have been used to increase the sensitivity of optoacoustic detectors [13]. Etalons act as resonators to amplify the intensity of the reflected optical signal.

Piezoelectric materials have been widely used as transducers since their discovery decades ago [11]. When a strain is placed on the atomic lattice of a piezoelectric material, changes in the atomic spacing of the lattice generates an electric field. Therefore, pressure waves colliding with a piezoelectric material will cause a measurable electric field to be generated. The reverse is true as well. Accordingly, when a piezoelectric material is exposed to an electric field, pressure waves are emitted. This makes piezoelectrics ideal for both producing and receiving ultrasonic waves. Due to their nature, the sensitivity of a piezoelectric transducer can be increased with their size.

Although alternate types of transducers have their merits, a piezoelectric transducer is optimal for VALIS. Capacitive transducers are not optimized for the high frequency ultrasonic waves that will be produced from the photoacoustic effect. Meanwhile, optical ultrasonic measurements require many additional optical components and higher complexity, leading to increased costs. On the other hand, piezoelectric ceramics are commonplace in sonography, making them frequently fabricated components and more readily available.
Generally, a linear array transducer is made up of four primary components: the backing, piezoelectric material, acoustic matching layers, and acoustic lenses [14]. The industry standard fabrication technique is the dice and fill method. First, a bulk piezoelectric material is mechanically diced [15]. Next, a highly acoustically attenuating material is inserted between the transducer elements to reduce ring-down, cross-talk between neighboring array elements. This makes the piezoelectric material into an array. The acoustic matching layers act to raise the transmission efficiency of the transducer. Similar to optical lenses,

acoustic lenses are able to focus or diverge incoming acoustic signals. Aside from focusing the ultrasonic waves for transducers, the acoustic lenses play another important role. They protect the acoustic matching layers [16]. Lastly, the backing layer acts to absorb any remaining ultrasonic waves. Figure 3.2.1 shows an assembly of the major parts that make up a typical piezoelectric transducer array.

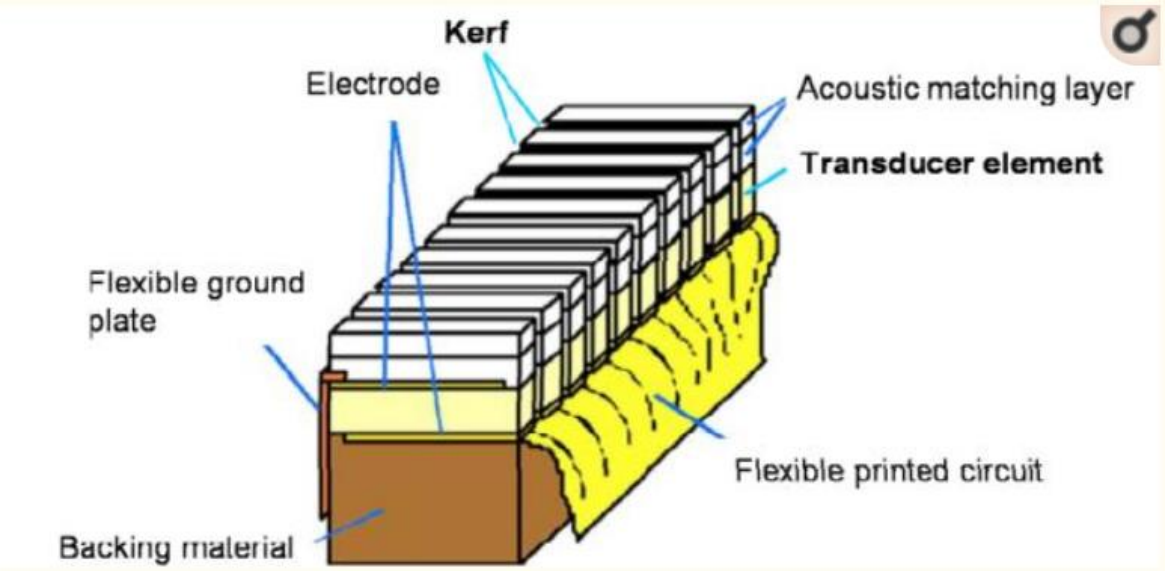

Figure 3.2.1: Schematic diagram of linear array transducer [15]

The transducer geometry affects the image quality within different planes and the area that can be imaged. Some examples of geometric variations for transducers include spherical scanners, cylindrical scanners, and planar scanners which can be seen in figure 3.2.2 [8]. The limitations of the cylindrical or spherical detections are apparent as these geometries are limited to small subjects due to their requirement for accessing all points around the target. For these reasons, the optimal transducer design parameter of our application of PAT will be achieved with the implementation of planar scanners

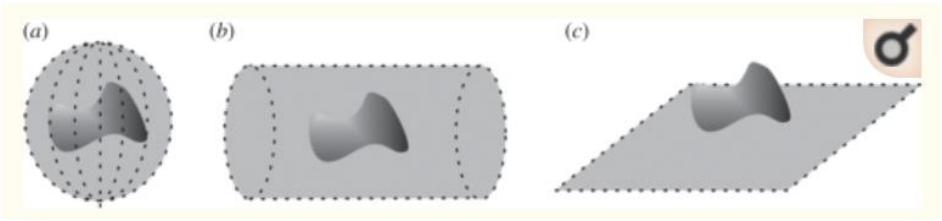

Figure 3.2.2: PAT detection geometries (a) Spherical, (b) cylindrical and (c) planar [8]

The planar detection geometry has its strengths, providing more versatility which then can be implemented into a mobile hand-held array probe. This is very suitable for our target market of researchers. Planar detection methods can implement a single-element ultrasound transducer and a linear array transducer. We will be using a linear array transducer set up, as single element transducers have long image acquisition times [8]. A PA image can be reconstructed by merging all data acquired from each transducer element, with large acceptance angles within the field of view [17].

The axial resolution produced from acoustic waves is dependent on the transducer frequency and bandwidth [10]. In the case of PAI, the frequency produced by the absorber is related to the boundary geometry of the absorbing tissue. An absorber on the scale of a few hundred micrometers will generate ultrasonic waves approximately in the ranges of 400 kHz to 20 MHz. In contrast, an absorber on the ranging a millimeter across would produce ultrasonic waves roughly in the range of 70 kHz to 2.5 MHz [4].

Transducers with frequencies approaching 100 MHz are able to provide resolutions on the scale of tens of micrometers. Higher frequency signals however, are subject to higher levels of attenuation. However, transducers with lower frequencies provide lower axial resolutions, but experience less acoustic attenuation and are capable of detecting signals from deep-lying absorbers [18].

For our application of photoacoustic tomography, utilizing transducers with lower frequency is best suited. Transducers with frequencies below 10 MHz are commonly used in PACT systems to provide an imaging depth greater than 1cm [17]. We plan to take advantage of existing, commercially available ultrasound scanners with the frequency range between 2-8 MHz as an inexpensive means of implementing PA imaging [8]. Table 3.2.1 summarizes the system characteristics of a typical PA system.

Modality	Lateral resolution (μm)	Axial resolution (μm)	Imaging depth (mm)
Subwavelength OR-PAM[76]	0.22	15	0.1[a]
Second generation OR-PAM[31]	2.5	15	1.2[a]
Dark-field AR-PAM[34]	45	15	3[a]
Bright-field AR-PAM[77]	44	15	4.8[a]
Spherical-view PACT[46]	420	420	53[b]
Cylindrical-view PACT[48]	100–250	100	10[a]
FPI PACT[62]	120	27	10[a]
Clinical linear array PACT[11,78]	720	640	70[b]

Note: FPI: Fabry–Perot interferometer.

[a]Based on in vivo data.
[b]Based on phantom data.

Table 3.2.1 Summary of typical PA system characteristics [8]

The operating temperature consideration for the transducer has been noted; however, the piezoelectric crystal will determine the usable temperature range as well as the operating temperature. Observing the experiment conducted to view the temperature rise in linear array transducers during use, the center of the front face surface on the linear array was found to heat up by 19K after 200s. [19] A graph of the temperature rise from the experiment is shown in figure 3.2.3.

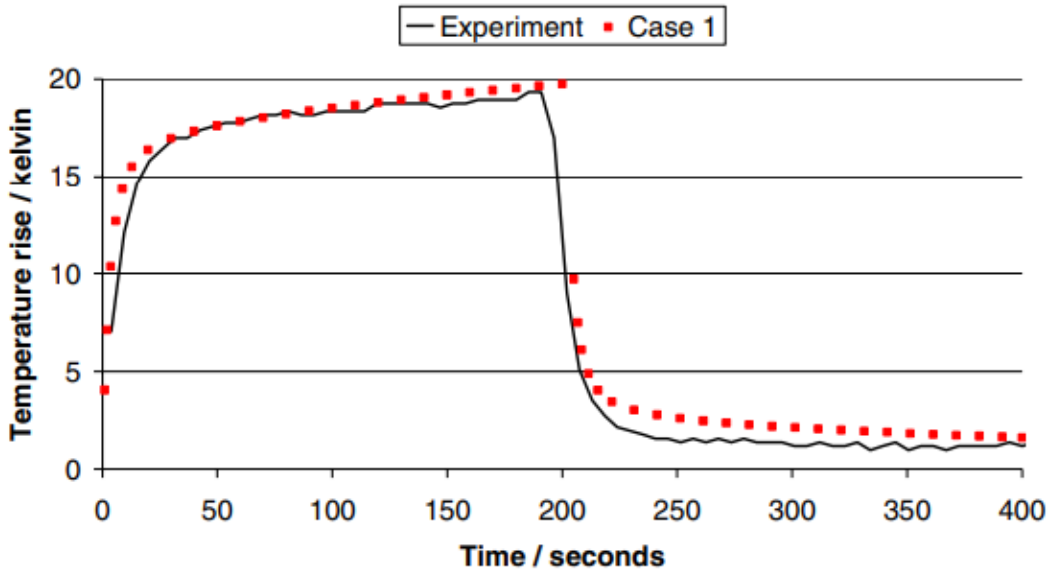

Figure 3.2.3: Comparison between the measured temperature rise at the centre of the surface from thermography and that predicted by case 1; the best fit model. [19]

Since transducer arrays can contain quite a few elements, a common method for receiving only a few signals at once is to turn on a small group of transducer elements at once. By rapidly changing the group of transducers that are active an image can still be created in real time.

The relevant design specifications for the transducer are outlined in table 3.2.2 shown below.

Design ID	Design Specification
Des. 3.2.1-C	The probe should be used in planar detection geometry for accurate data collection
Des. 3.2.2-C	Must be implemented with a linear transducer array
Des. 3.2.3-C	The transducer will be made from piezoelectric materials
Des. 3.2.4-C	The frequency range should be between 2-8 MHz 100% -6dB bandwidth

Table 3.2.2 Design requirements for the transducer

3.3 DAQ

3.3.1 Overview and Interfacing

At a high level, the roles and requirements of the processing computer, the user, and the hardware system can be seen in Figure 3.3.1. Outlining the relationships in this manner motivates the formalization of tasks and permissions afforded to each entity, and the communication that must occur between them.

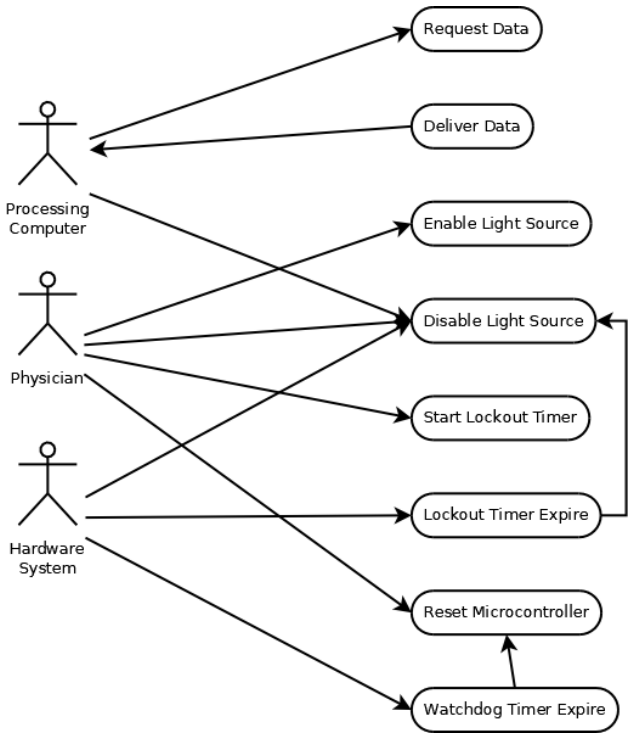

Figure 3.3.1: DAQ Use Case Diagram

For the processing computer to communicate with the DAQ, it must use a USB serial interface with flow control (RTS/CTS) running at 1Mbps with 8 data bits, 1 stop bit, no parity, LSB first. Figure 3.3.2 details the preliminary communications protocol between the DAQ and the processing computer. All communications are sent as ASCII with space parameter separation and line feed termination (‘\n’), except for transfers of samples which are sent as little endian 8-bit binary. Return codes are two digits followed by a line feed. Interfacing programs will need to store a table of status code to string conversions.

The transaction starts with the processing computer sending the command opcode, and any associated parameters. The DAQ will analyze the incoming command and determine whether it is valid or invalid and send a receive acknowledgement. If the command is malformed, it returns an invalid command status. Otherwise, it sends an acknowledgement of command reception. The DAQ will then attempt to run the command. If there is an error during this process, the DAQ will return a failed command status. Otherwise, it will return a successful command status. If there is any data associated with the command, it will send this as binary and append a 16-bit data CRC. The processing computer must respond with a data acknowledgement to confirm a successful transfer.

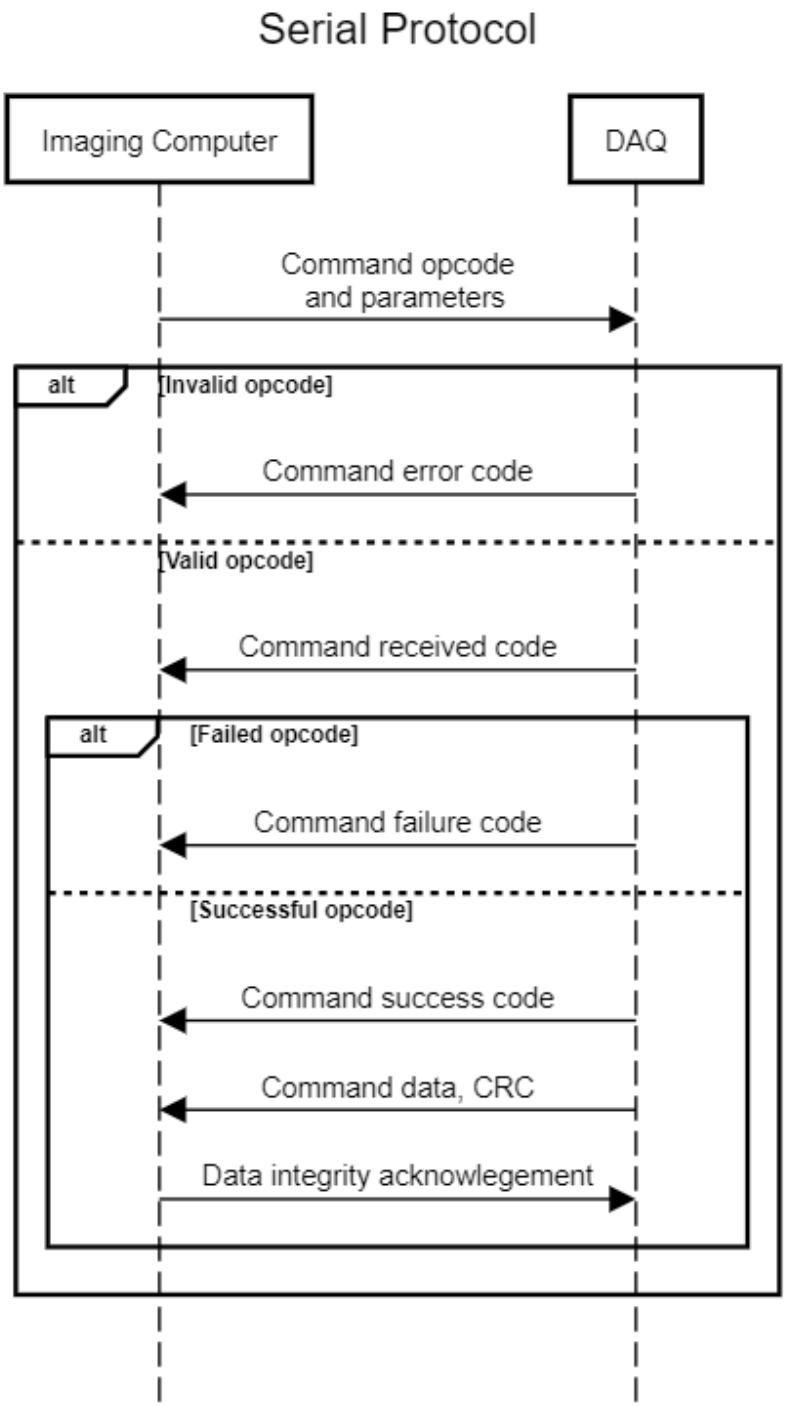

Figure 3.3.2: Serial Communications Sequence Diagram

3.3.2 Hardware

The DAQ schematic, shown in figure 3.3.3, details the communications occurring between the core circuit components; namely, the transducer amplification and filtering, the signal conditioning, the microcontroller, the safety lockout, the RS-232/USB converter, and the computer itself.

The incoming signal from the transducer section will have already been subjected to amplification and bandpass filtering to ensure the signal integrity, and only contains the relevant frequencies pertaining to the transducer effective range.

The main peripheral of the system is an 10-bit Analog-Digital Converter (ADC) MCP3008. This is an SPI compatible ADC with 8 input channels with a maximum sample rate of 20khz. The incoming transducer signal is a continuous analogue voltage corresponding to the distances of the ultrasound waves. To be able to store these on the microcontroller, it must first be discretized by the ADC into samples. Analog multiplexers are used to create a multiplexer chain, which is used to allow multiple signals to feed into the same ADC.

At the heart of the system is the AT89S8253 microcontroller. It is an 8051 architecture controller with dual UART & SPI capabilities. In its basic form, the microcontroller acquires the discrete samples by the ADC, and relays them to the imaging computer. For a more efficient design, the samples are sent concurrently to receiving them. Otherwise the microcontroller would require more memory to store all the samples, which would drive up the cost. The microcontroller will also receive safety sensor data in case an emergency shutoff is required. It will also control debugging LED and a buzzer for user feedback.

The safety lockout consists of several user inputs and state sensors to prevent unsafe LED actuation. User input comes in the form of a probe enable button and a contact sensor to mitigate accidental actuation. The possibility of excessive heat and current necessitate the inclusion of temperature and current sensors to lockout the device in this eventuality. It is important to note that the safety interlock devices must be able to work independently of the microcontroller; in the event of lockup, the microcontroller would not be able to service the safety systems, rendering them useless in preventing unsafe usage.

To communicate externally, the MAX3232 RS-232 level shifter and CP1202 Serial-USB converter (not pictured) will be used. In the proof of concept only the level shifter will be used, and an RS-232 to USB cable will serve the CP1202's place. In later designs, a usb socket will be available. A RS-232/USB converter serves as an intermediary between the microcontroller and the imaging computer, completing the data acquisition process. It simplifies the USB design process as the heavy lifting can be done in a black box circuit while the microcontroller can benefit from the simplicity of RS-232.

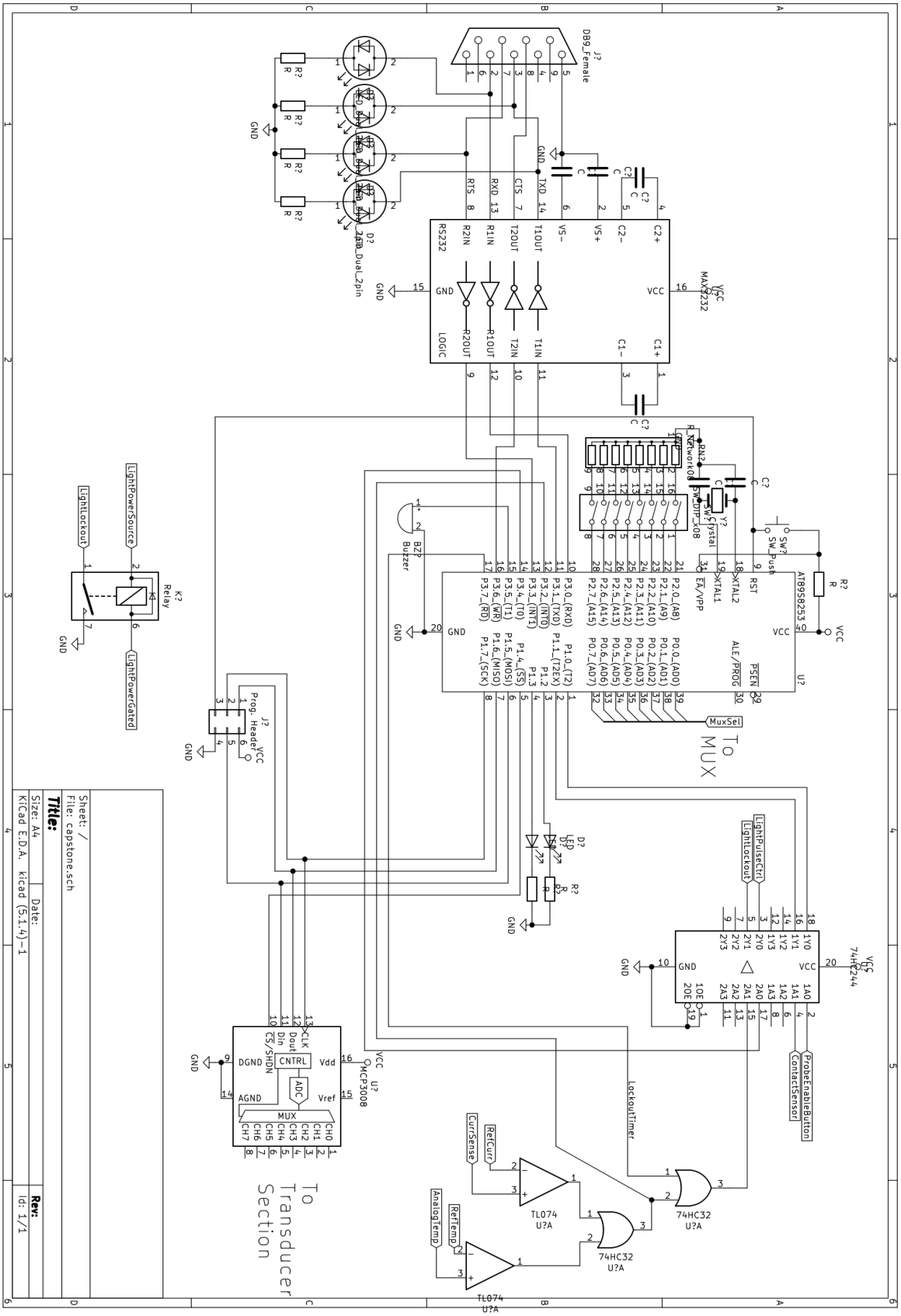

Figure 3.3.3: Detailed DAQ schematic

3.3.3 Firmware

The firmware component employs an interrupt-driven design. Whenever a component requires attention, it will alert the microcontroller, which will stop execution of the main program and start servicing the component. The system will service interrupts from the following sources (interrupt name in parenthesis):

- Imaging Computer Serial Communication (Serial)
- ADC SPI Communication (Serial)
- Emergency Shutdown (INT0)
- Imaging Computer CTS disable (INT1)

When the DAQ is out of reset, it will start execution of the main program shown in figure 3.3.4. It will preload any variables and read the settings eeprom which will contain non-volatile configuration data. It will then enable interrupts and start the program loop. In this loop, it will constantly poll for changes in inputs, update timers if required, check if a command has been received and requires processing, and whether a sample needs to be written out to the UART. In the implementation, this may be written as the flowchart, or utilize an event queue to increase code modularity in case of future amendments.

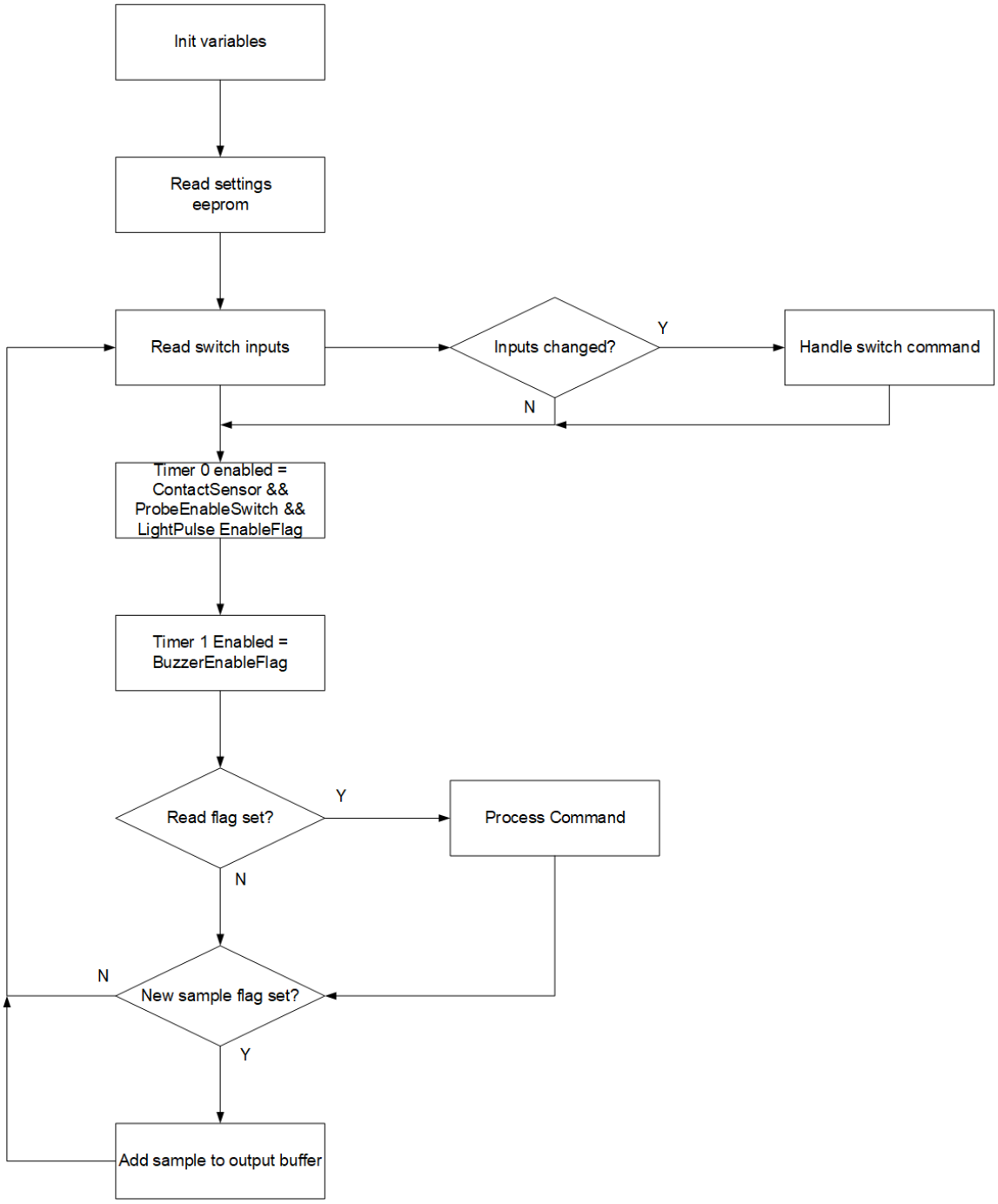

Figure 3.3.4: Main Program ISR Flowchart

The Serial interrupt , described in figure 3.3.5, can be triggered three different ways: SPI byte sent, UART byte sent, and UART byte received. The Serial interrupt must check within status registers to determine which source raised the interrupt. For SPI, the ADC command will have finished so it will collect the sample and reload a new command if needed. For byte received, it will check if it is the command terminator, and set a flag if it is. Otherwise it will store the character in the input buffer if it is not full. For byte sent, it will reload the next character to be sent, if any.

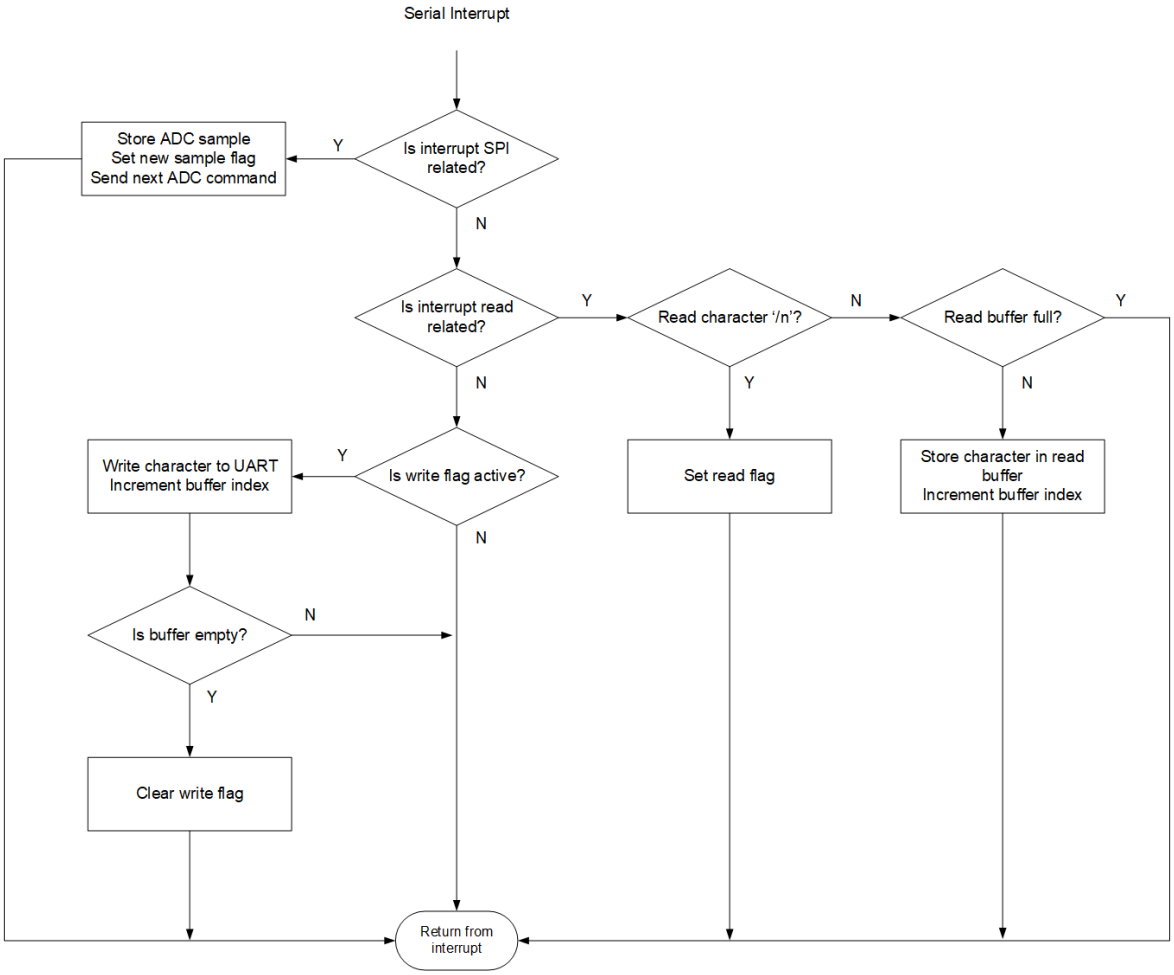

Figure 3.3.5: UART & SPI ISR Flowchart

The emergency shutoff flowchart shown in figure 3.3.6 is triggered by the temperature sensor or the current sensor. If either of these exceed a safe value, an interrupt will be raised. Although the lockout will activate regardless of the microcontroller, it will permanently disable the power to the light source and sound an alarm until the system is reset so the operator can be made aware of the situation and handle it accordingly.

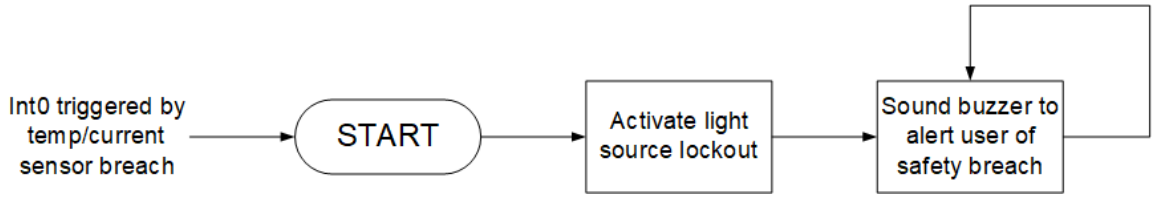

Figure 3.3.6: Emergency Shutoff ISR Flowchart

All the important design requirements for the DAQ unit are displayed in table 3.3.1.

Design ID	Design Specification
Des. 3.3.1-C	ADC must produce a reliable sample up to 8-bit, which is read from the analog transducer value.

Des. 3.3.2-C	DAQ circuit consists of signal conditioning components, MCP3008, AT89S8253, and MAX3232.
Des. 3.3.3-P	Circuit will be housed in a protective rigid casing.
Des. 3.3.4-P	Desired sample rate of transducers cannot exceed 200kHz / # transducers.
Des. 3.3.5-P	Sample export rate must be faster than ADC sampling rate.
Des. 3.3.6-C	All hardware components must be readily orderable parts.
Des. 3.3.7-C	AT89S8253 has a USB-compatible interface.
Des. 3.3.8-F	Microcontroller uses USB to communicate with the imaging software computer.
Des. 3.3.9-P	DAQ contains a watchdog that will reset after 1ms of inactivity.
Des 3.3.10-P	Light source can only be operated when the probe enable button is pressed and the contact sensor is applied.
Des 3.3.11-P	Excessive readings from either temperature sensor or current sensor break the light's power source. This will function independent of the microcontroller.

Table 3.3.1 Design requirements for the DAQ

3.4 Peripheral Hardware

In addition to the hardware required for the light source, transducer, and data acquisition unit, smaller circuitry must be included in order to protect the various elements. It will also improve the safety of the device and considerations for the power supply of the device must be taken. These safety considerations include proximity sensors, temperature control, voltage and current limiting, and finally sufficient grounding. All these features will require independent circuitry and separate testing in order to validate the performance.

It is an important safety feature to restrict the light source from turning on while it is not in contact with a surface to be imaged. This can be achieved using infrared (IR) LEDs as well as a IR sensor to detect the distance from the object. The IR LEDs continuously emit light which is reflected by surfaces in front of it, and the reflected light is detected by the IR sensor. The magnitude of the light reflected is used to determine the distance of the sensor from an object. For use on humans and other living things, the IR radiation given off by them must be considered in the determination of distance, and should be able to be corrected for by adjusting the magnitude detected for the average magnitude of IR radiation given off by the subject per unit of area. Fortunately, the radiation given off by living creatures and people is typically deeper in the IR spectrum. Therefore, using a NIR LED for the proximity center will likely reduce the risk of the radiation interfering from the subject being imaged. This circuitry can be controlled through a microcontroller. In order to ensure the LED does not be considered in the calculation for our MPE, the power of the IR LEDs being distributed to the subject must be sufficiently small, less than 200 mW. Also, to reduce the MPE of the subject from the IR LEDs, and to ensure little interference with the light source, the wavelength must be between 850 nm and 950 nm.

In addition to this, temperature of the light source must be considered for the safety of the patient and the user performing the scan. For this, a temperature sensor, heat sinks and a small fan can be employed in order to ensure the temperature is at safe levels. These elements can also be controlled by the microcontroller to monitor and adjust the temperature. To ensure the device can be used for enough time to successfully acquire images, the temperature control should keep the temperature below maximum levels for at least 10 minutes of constant use. The maximum temperature that should not be exceeded should consider the various system components as well as the safety of the patient and user. The temperature at which the device has the potential to injure the patient is much lower than the maximum of the components and will be considered for the max temperature. Limiting the temperature to 60ºC keeps the risk of burn relatively low, much lower than the temperature which burns appear quickly [20]. In order to accurately detect the temperature of the enclosure, the temperature sensor must be able to detect a range of temperature from 0 to 100ºC. Both of these safety features can be seen in the below circuit diagram in figure 3.4.1.

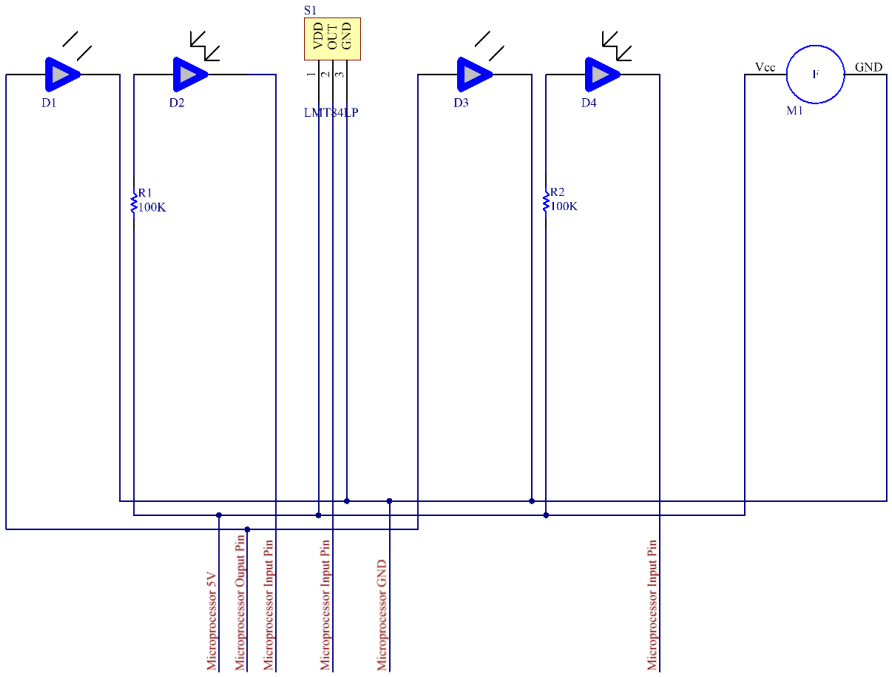

Figure 3.4.1: The preliminary design for the proximity sensor and temperature control, both of which can be run by a microcontroller

Another important safety consideration for the device is the current through the LEDs. This is important to limit the current in the event of a short circuit to protect the patient and professional, as well as to protect the LEDs in the interest of sustainability. This current protection can be achieved through a feedback loop of transistors and a resistor, which will constantly monitor the current through the LEDs. In the event of a high current, the transistor completing the circuit and connecting the LEDs to the ground will be disconnected, protecting the circuit from overcurrent. The signal being used for pulsing the light source, originating from a microcontroller, will be diverted through the second transistor to ground, bypassing the first transistor. The limit of the current through the LEDs can be modified through changing one resistor in the circuit. This circuit will also allow a microcontroller to pulse the light source at the desired frequency, as the transistors have a fast rise and fall

time. In order to achieve a pulsing of at least 100 ns the total rise time and fall time of the transistor must be at most 10 ns.

Along with the consideration of the circuitry protection, another important part to consider for the safety and operation of the LEDs is the power supply. Each LED has a power rating of 10 Watts, and the power supply should be sufficient to offer room for overdriving the light source. Along with the power, the voltage and power must be within the operating range of the LEDs. In this case, a sufficient power source is required to offer at least 200 Watts of power, with a maximum voltage in the range of 12.5 V to 16.8 V and a current in the range of 10 A to 16 A. In addition to these requirements, the power supply should have the ability to be powered by a North American wall outlet, capable of converting 120 VAC at 60 Hz to the required DC voltage. The proposed circuit diagram for the powering, control and protection of the LEDs can be seen in figure 3.4.2.

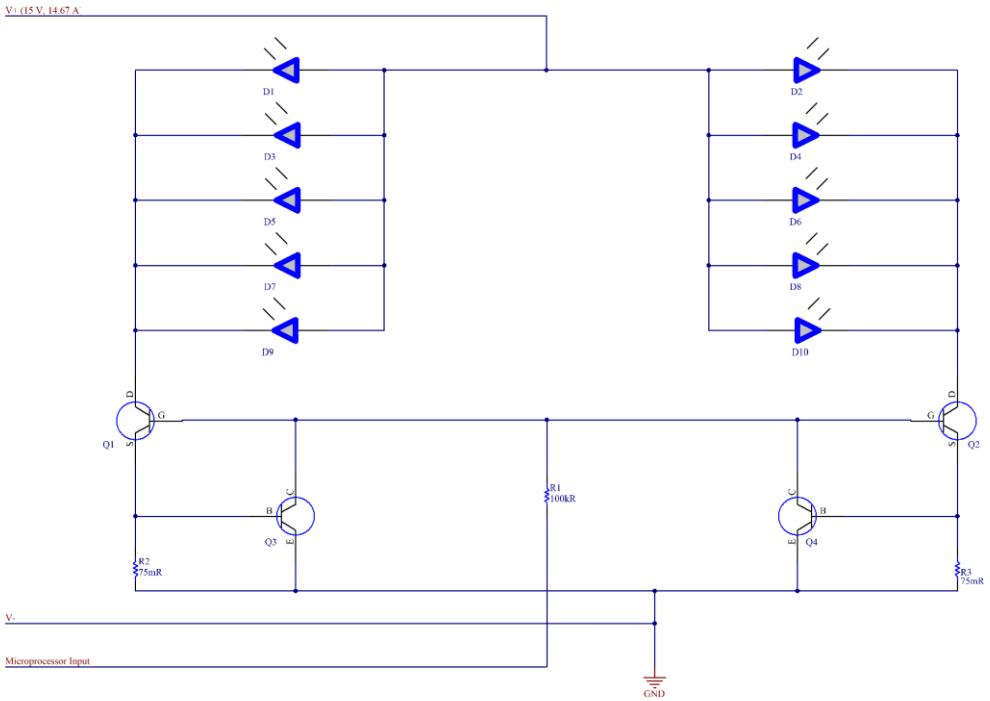

Figure 3.4.2: The circuit for protection for the LEDs limiting the current

Finally, for the safety of the users and patients it is important to have a grounding unit around the enclosure of the high-power circuitry. Because the LEDs require approximately 10 Watts each, it is important to isolate them from the users through the use of an enclosure ground. This can be completed by running a conductive medium around the body of the enclosure and connecting this to the ground of the power. In the event of the short circuit or failure of components, the enclosure ground will offer a safe path to ground rather than through the user or the patient. This is achieved with a metal encasing around the enclosure offering an electrical barrier between the components and the users. The design specifications are contained in table 3.4.1.

Design ID	Design Specification
Des. 3.4.1-P	The light source will only turn on if the device is within 1 cm of the object to be imaged
Des. 3.4.2-P	IR LEDs for proximity sensor will have power less than 200 mW
Des. 3.4.3-P	IR Leds for proximity sensor will have a wavelength between 850-950 nm
Des. 3.4.4-P	Proximity sensor must account for IR radiation given off by subject when calculating the magnitude of IR light reflected
Des. 3.4.5-P	The internal temperature of the device will be limited to 60ºC
Des. 3.4.6-P	In the event the temperature exceeds maximum limitations the device will turn off until temperatures are within usable limits
Des. 3.4.7-P	The device will remain under the maximum temperature while being used continuously for at least 10 minutes.
Des. 3.4.8-P	The temperature sensor will be capable of sensing temperatures from 0 to 100ºC
Des. 3.4.9-C	The current through the LEDs will be limited to 1.5 A
Des. 3.4.10-C	The voltage coming out of the power supply will be limited to 150 V
Des. 3.4.11-C	The rise time of the transistors in the light source current limiting loop will be less than 10 ns
Des. 3.4.12-C	The fall time of the transistors in the light source current limiting loop will be less than 10 ns
Des. 3.4.13-C	The power supply will supply at least 200 W, with a voltage range of 12.5-16.8 V and a maximum current of 10-16 A.
Des. 3.4.14-C	The power supply will be capable of being powered by North American wall outlets, accepting 120 VAC at 60 Hz
Des. 3.4.15-P	The device enclosure will be grounded to ensure safe use of the device

Table 3.4.1 Design requirements for safety circuitry and circuit protection

3.5 Signal Amplification and Filtering

Before any processing, the signals produced by the transducer will be filtered and amplified. Figure 3.5.1 shows a schematic for a two-stage amplifier with a bandpass filter, and figure 3.5.2 shows a proposed voltage gain selector. Each amplifying stage consists of a non-inverting amplifier with a bandpass filter added to the second stage. High frequency op amps will be used to ensure there is no degradation in the performance of the amplifying and filtering circuitry.

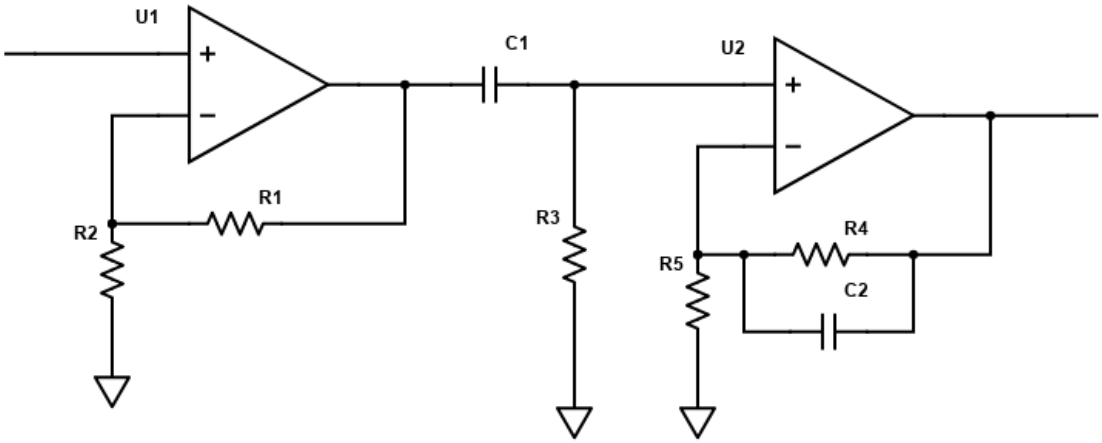

Figure 3.5.1: Two stage amplifier and filter for received signals from the transducer

The bandpass filter will attenuate frequencies just outside of the effective range of the transducer and the overall voltage gain of the two stages will exceed 40 dB. The signal will get a positive DC voltage offset to ensure an entirely positive signal is passed through the ADC and none of the signal is truncated. To prevent the possibility of any current being drawn from the input of the ADC, a diode will be placed prior to the input pin of the ADC.

The circuit in Figure 3.5.2 shows the voltage reference selector. This circuit is essentially a precision voltage divider followed by the regulation of this voltage. The input voltage will be a constant regulated voltage, and the microcontroller can select what reference will be fed into the ADC. This has the effect of reducing the full-scale voltage of the ADC, which results in a “gain” of the input signal by making each output bit worth less of the input. The case when all multiplexer inputs are 0 removes the voltage divider from the circuit, and uses the regular voltage reference.

As this will increase the cost and complexity of the circuitry, for further prototypes we may elect to use ADCs that perform this internally, such as the PGA in the ADS1015. One caveat to this is that it has a significantly higher cost. Alternatively, the inputs to the ADC could be amplified rather than the reference. This circuit would use an inverting op-amp with multiplexed resistors rather than a voltage divider. The downside is that either the circuit needs to be replicated for as many channels on the ADC or the spare ADC channels go unused.

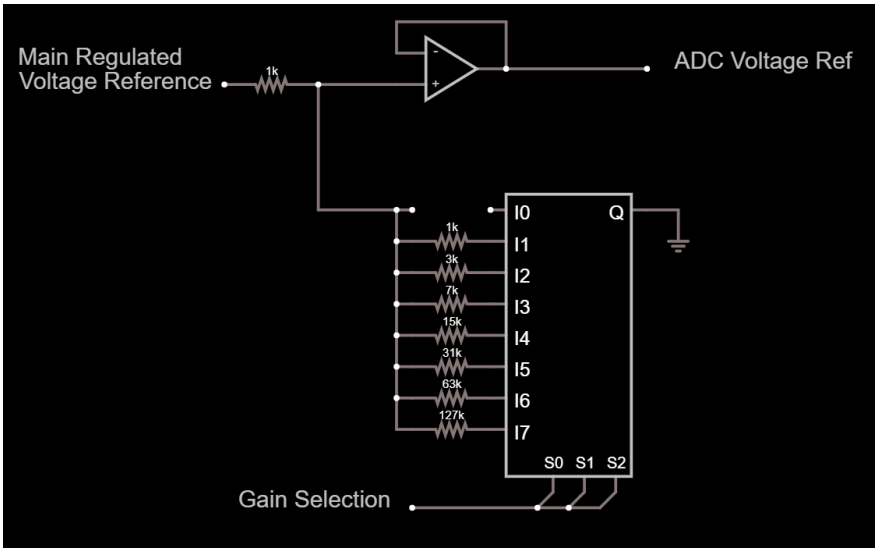

Figure 3.5.2: Voltage Reference Selector

The relevant design requirements for the signal conditioning before processing are outlined in table 3.5.1.

Design ID	Design Specification
Des. 3.5.1-C	The voltage gain from at least a two-stage amplifier will exceed 40 dB
Des. 3.5.2-C	The bandpass filter will attenuate signals outside the frequency range of the transducer
Des. 3.5.3-C	A diode will ensure there is no current draw from the ADC input pin
Des. 3.5.4-C	The op-amps must be operational with frequencies up to 10 MHz
Des 3.5.5-C	A DC voltage offset will be added to the transducer signal to prevent any loss of information at the ADC
Des. 3.5.6-P	There will be variable digital amplification

Table 3.5.1 Design requirements for signal conditioning

3.6 Device Enclosure

Along with the electrical components of the device, the device enclosure is another design aspect to be aware of. The device enclosure must be able to house the light source, light source control circuitry, proximity sensing equipment, temperature sensing equipment as well as the cooling apparatus. In addition to being able to house all of the required components, the device enclosure must also be able to be attached to the transducer, to situate the light source next to the transducer elements, and the proximity sensors close to the object being imaged. The enclosure should also act as a barrier between the user, the light source, and any electrical components. The design of the enclosure must be ergonomical to hold, light, temperature resistant, and finally cost effective.

To design a device enclosure that meets all of these requirements, the best solution is to 3D print a custom enclosure from PLA filament. The custom designed enclosure can house

all of the necessary components and can be made to attach to the transducer in an easy and secure manner. With proper design the enclosure will also meet the requirements of being ergonomical and light, and 3D printing materials are a very cost-effective method of developing prototypes and creating custom designs. Finally, the printed PLA filament will be able to withstand the maximum temperatures outlined in section 3.4, 60ºC. It will withstand these temperatures because the glass transition temperature, the temperature at which a material loses its hardness and begins deforming, of PLA is 65ºC [21]. In addition to this 3D printed enclosure, a grounded shield will be part of the enclosure to provide electrical insulation, and to provide the necessary shielding of the light source and electrical components. All the relevant detailed design specifications for the device enclosure are provided in table 3.6.1.

Design ID	Design Specification
Des. 3.6.1-P	The enclosure will house the light source, light source control circuitry, proximity sensing equipment, temperature sensing equipment and cooling apparatus.
Des. 3.6.2-P	The enclosure will be able to be attached to the transducer in a secure fashion
Des. 3.6.3-P	The enclosure will situate the light source close to transducer elements
Des. 3.6.4-P	The enclosure will be able to situate the proximity sensor in a position to detect the distance of the subject from the device
Des. 3.6.5-P	The enclosure will be ergonomic, comfortable, light and cost effective
Des. 3.6.6-P	The enclosure will insulate and shield the light source and electrical components from the user
Des. 3.6.7-P	The enclosure will be able to withstand temperatures of 60ºC
Des. 3.6.8-P	The enclosure will be sufficiently grounded to ensure the safety of the user and subject

Table 3.6.1 Design requirements for device enclosure

3.7 Image Processing and Reconstruction

3.7.1. Unfiltered Backprojection

The net result of the aforementioned tissue excitation, ultrasound sensing, and data acquisition components is a discrete dataset. However, further processing must be applied before reasonable output resembling figure 3.7.1 can be achieved. Numerous reconstruction algorithms exist, the most prevalent being Filtered Backprojection (FBP) and Computed Sensing (CS). FBP is known to be the simpler of the two algorithms, whilst CS generally returns better results. Regardless of chosen methodology, backprojection features prominently, and must therefore be the first design consideration.

Figure 3.7.1: MRA generated vasculature phantom

Motivation for the backprojection algorithm comes from the parallel projection sampling employed by ultrasound acquisition, as demonstrated in figure 3.7.2.

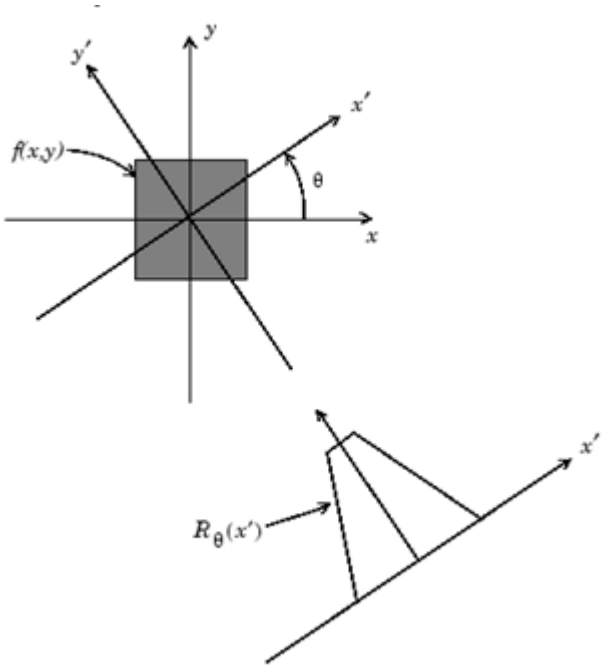

Figure 3.7.2: Physical representation of the Radon Transform [22]

As the ultrasound probe is rotated about the region of interest (ROI), the transducer elements receive pressure signals corresponding to depth information of the underlying vasculature tissue in the parallel plane. Acquiring tissue data in this manner results in a new intensity representation and mapping, relating the tissue locations and intensities to the angle of rotation. This representation can be replicated by using the Radon Transform, which maps the *f (x,y)* intensities and *x/y* locations to corresponding intensities and locations with respect to *x', y',* and *θ.* The Radon Transform is given by equation 5.

$$R(x',\theta) = \int_{-\infty}^{\infty} f(x'cos\theta - y'sin\theta, x'sin\theta + y'cos\theta)dy'$$

Equation 5. Radon Transform [23]

Using MATLAB, the Radon Transform can easily be applied to the target image to generate its corresponding transducer output as shown in figure 3.7.3. This closely resembles the expected initial dataset, on which the image reconstruction will be performed.

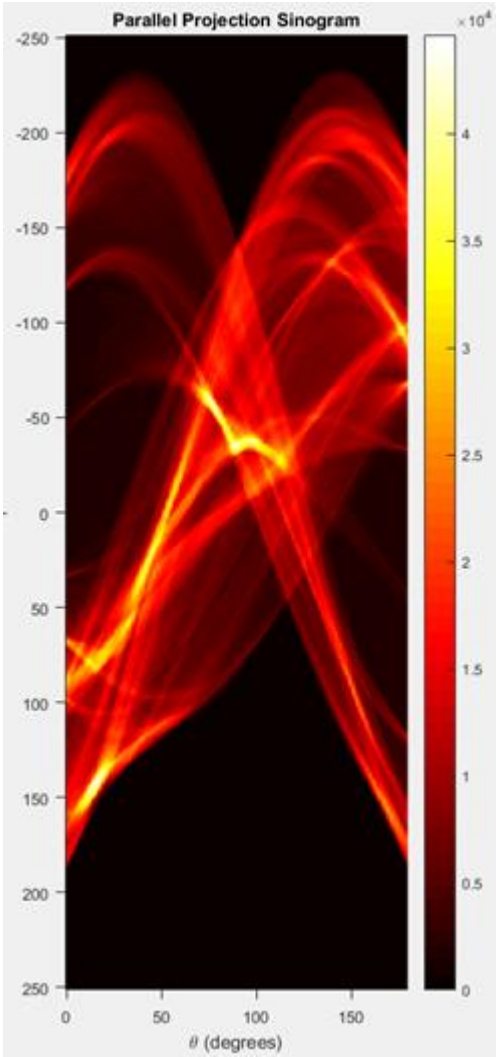

Figure 3.7.3: Sinogram of MRA generated vasculature phantom

Given the sinogram output of the ultrasound transducers, backprojection can intuitively be performed using the Inverse Radon Transform to project the samples taken about the ROI into a common plane, thereby providing the initial image reconstruction. Equation 6 represents the Inverse Radon Transform, used to remap the intensities to Cartesian coordinates.

$$f(x,y) = \int_{0}^{180} R(xcos\theta + ysin\theta, \theta)d\theta$$

Equation 6. Inverse Radon Transform [23]

Applying the Inverse Radon Transform to the Sinogram yields the vasculature phantom reconstruction shown in figure 3.7.4. Though the vasculature shape is apparent, the reconstruction leaves much to be desired. The image appears unevenly boosted due to oversampled high-density centers and unweighted sample summations. Blurring at the edges of the vasculature is indicative of poor intensity interpolation between pixel locations. These characteristics are practically unavoidable using backprojection; Thankfully, both can be corrected for after the initial image reconstruction.

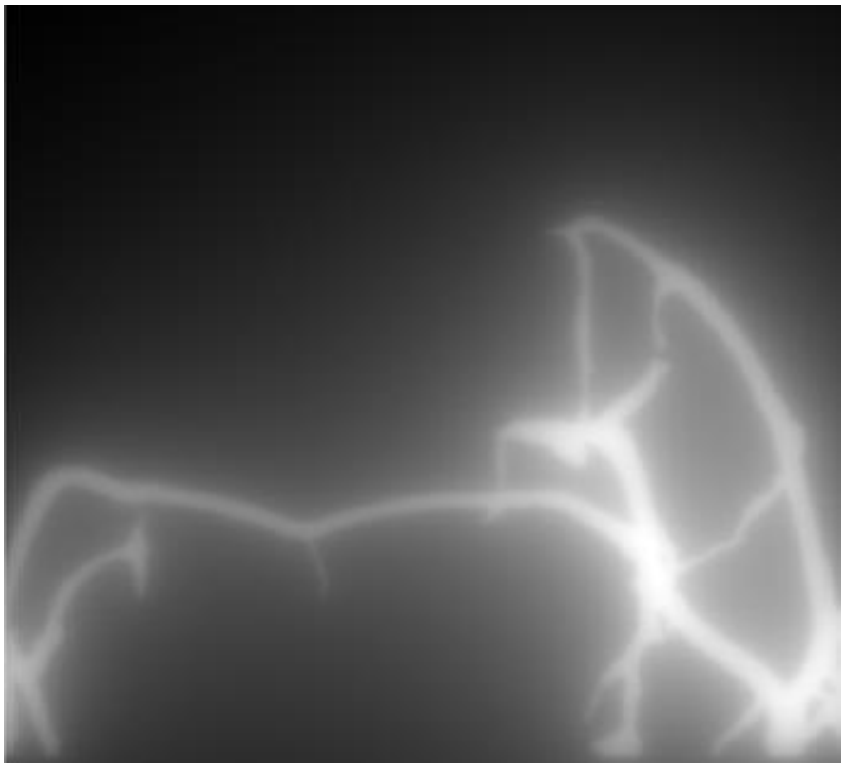

Figure 3.7.4: Unfiltered backprojection of MRA generated vasculature phantom

3.7.2. Filtered Backprojection

The simplest means of image correction is through application of a filter, by convolution in spatial domain or multiplication in frequency domain. There are several filters that are suitable for differing cases, as outlined in table 3.7.1 and figure 3.7.5. An application of a Hamming Window can be observed in figure 3.7.6, correcting the characteristic affectations of unfiltered backprojection with some success.

Filter Name	Description	Effect
Ram-Lak	Cropped ramp filter, infinite sampling	Best information retention but minimal noise reduction
Shepp-Logan	Multiplies the Ram-Lak filter by a sinc function	Increasing amounts of filtering down the table, with decreasing information retention and resolution as a result.
Cosine	Multiplies the Ram-Lak filter by a cosine function	
Hamming	Multiplies the Ram-Lak filter by a Hamming window; scaled cosine multiplier	
Hann	Multiplies the Ram-Lak filter by a Hann window; scaled cosine multiplier	

Table 3.7.1 Description and effect of backprojection filters [24]

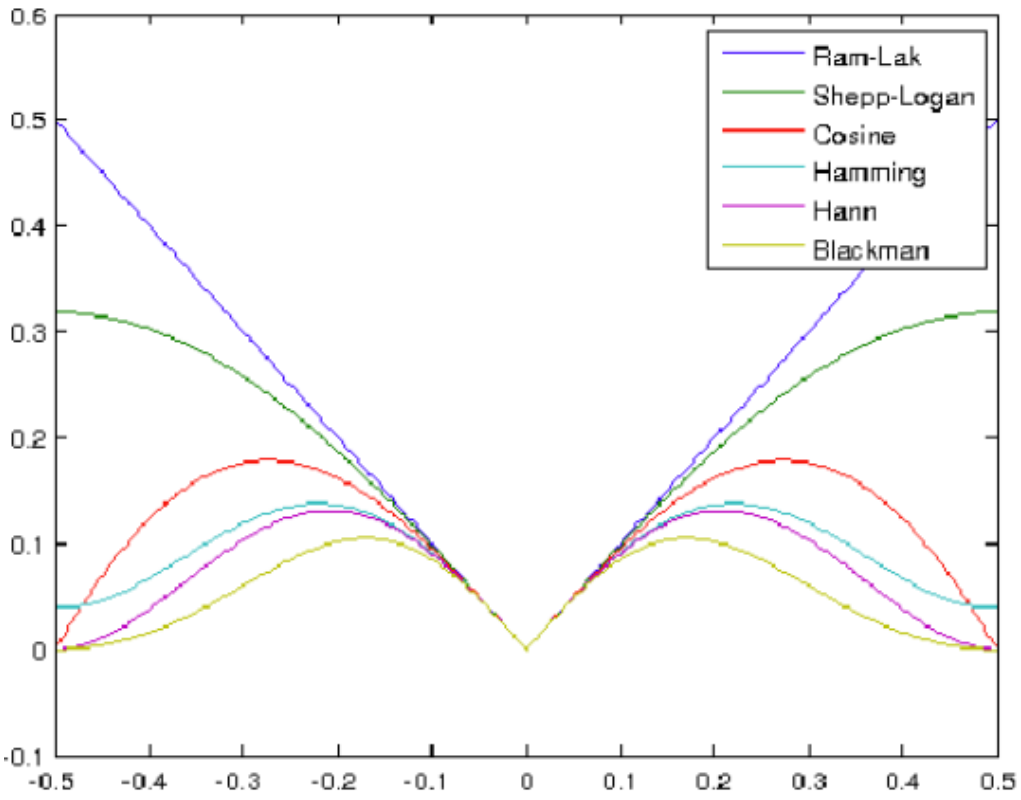

Figure 3.7.5: Frequency domain plot of backprojection filters [25]

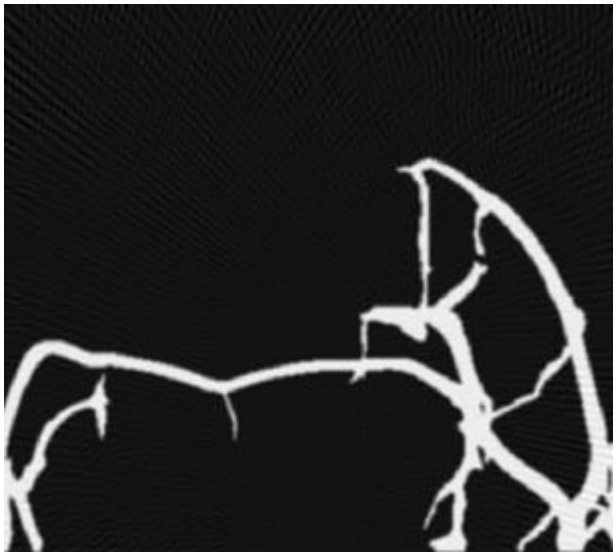

Figure 3.7.6: Hamming filtered backprojection of MRA generated vasculature phantom

From this image, the intensity equalization and deblurring effect of the Hamming Window filter become apparent. Image filtration is generally capable of producing higher quality results if the specific image defect is known, but therein lies the inherent disadvantage of FBP: no single filter will be applicable for all cases and thus the algorithm will always require some user intervention. This serves as the motivation for computed sensing.

3.7.3. Computed Sensing

Much like FBP, Computed Sensing commences with an application of unfiltered backprojection as a starting point. However, the reconstruction scheme soon becomes much more elaborate, as shown in figure 3.7.7.

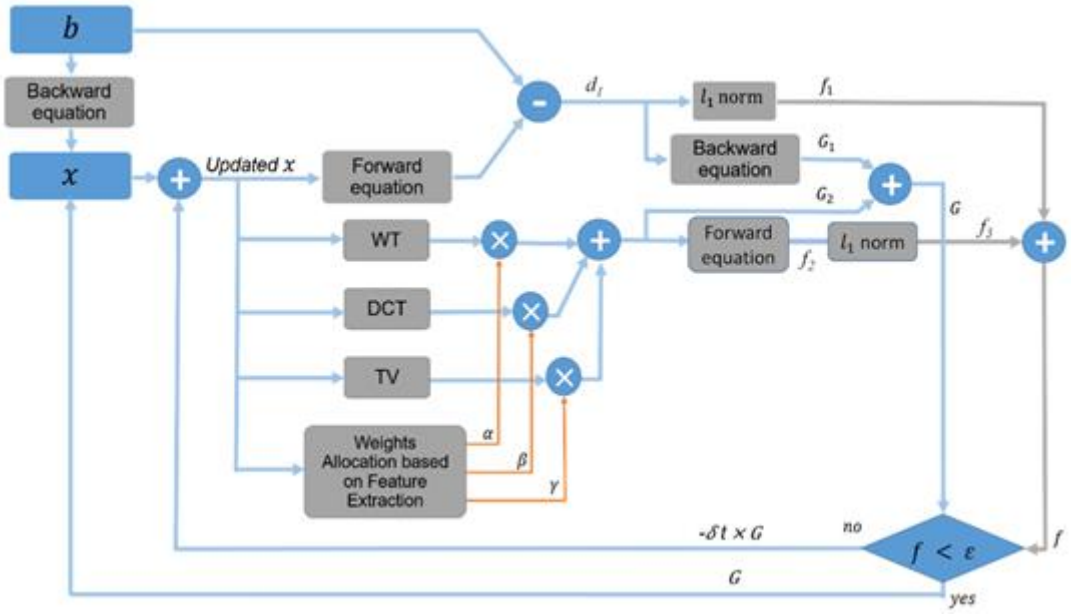

Figure 3.7.7: Flowchart detailing the Computed Sensing algorithm [26]

Employing several weighted sparsifying transforms, the algorithm isolates the most crucial pieces of information from the backprojection. The weighted summation of sparse slices is compared to the reference image of each iteration, repeating until the norms are minimized; this is to say, the algorithm will run until the difference between subsequent trials is minimal, at which point it will have converged upon a solution. Alternatively, the algorithm can be made to run until the error is less than that specified by the user, which is useful in decreasing execution time if a less-than-perfect solution is acceptable.

At the core of the CS algorithm are the sparsifying transforms used to extract important details; namely, the Wavelet Transform (WT), the Discrete Cosine Transform (DCT), and the Total Variation (TV.) Each of these three transforms emphasizes a different characteristic, and the user retains the ability to scale these characteristics differently depending on the desired detail.

The Wavelet Transform operates on the premise of using finite wavelets to isolate and remove noise figments in the Fourier domain, leaving the rest of the signal intact. Wavelets can be scaled and shifted to align with specific features which are present in the infinite Fourier sinusoid, and can thus be used to condition the signal in a localized manner. Thus, the remainder of the image does not experience detrimental side effects. The definition of the Wavelet Transform is dependent on the specific wavelet used.

The Discrete Cosine Transform, defined by equation 7, is commonly used to perform image compression by reducing its representation to a set of basis vectors and corresponding coefficients, in terms of horizontal and vertical cosines. In this specific application, reducing the entirety of the image to spectral sub bands allows the user to easily manipulate the DCT coefficients across all rows and columns, and highlight important image details.

$$X_{k_1,k_2} = \sum_{n_1=0}^{N_1-1}\left(\sum_{n_2=0}^{N_2-1} x_{n_1,n_2}\cos\left[\frac{\pi}{N_2}\left(n_2+\frac{1}{2}\right)k_2\right]\right)\cos\left[\frac{\pi}{N_1}\left(n_1+\frac{1}{2}\right)k_1\right]$$
$$= \sum_{n_1-0}^{N_1-1}\sum_{n_2-0}^{N_2-1} x_{n_1,n_2}\cos\left[\frac{\pi}{N_1}\left(n_1+\frac{1}{2}\right)k_1\right]\cos\left[\frac{\pi}{N_2}\left(n_2+\frac{1}{2}\right)k_2\right].$$

Equation 7. Discrete Cosine Transforms, applied across all rows and columns [27]

The Total Variation Transform, defined by equation 8, is simply the gradient field across an image, indicating areas of large change such as edges. Common methods of obtaining the gradient include kernel convolution across the surface using such filters as Sobel and Prewitt. This is especially useful for edge preservation, one of the most important aspects of image processing. This can be expanded upon using the Split Bregman denoising optimization problem, minimizing the sum of the L2 norm and the weighted total variation.

$$TV(y) = \sum_{i,j}\sqrt{\left|y_{i+1,j}-y_{i,j}\right|^2+\left|y_{i,j+1}-y_{i,j}\right|^2}$$

Equation 8. Total Variation, applied across all rows and columns [28]

Figure 3.7.8 provides a concise overview of Computed Sensing, using the WT and TV transform over 30, 60, 90, and 120 projections. Highly customizable by design, it is clear to see that Computed Sensing can greatly enhance image quality beyond the capabilities of simple FBP.

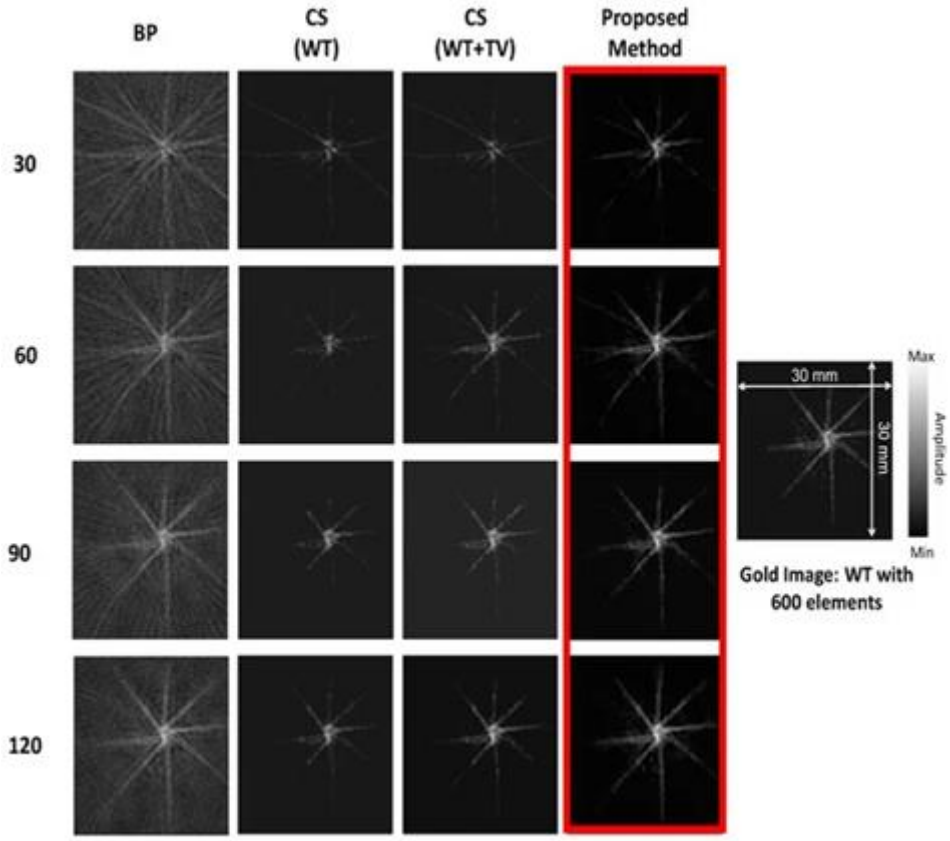

Figure 3.7.8: Comparison of simple BP and CS reconstruction methods [26]

From the design of the image reconstruction methods shown above, it is clear to see that there is no clear “right answer”; there are many factors contributing to the reconstruction quality, from the number of projections about the ROI to the sparsifying transforms utilized in detail extraction. Each input dataset will exhibit unique characteristics that the reconstruction suite will need to handle without excessive user consultation. Deciding which method is most suitable is a difficult task.

The FBP algorithm is favourable in that it is conceptually and computationally simple, and should work in near-real time to provide a consistent imaging stream. Unfortunately, the image reconstruction leaves much to be desired; Projections must be taken at very small (<10°) angular increments for acceptable resolution, and filtration options are limited. Remaining artifacts are removable, although subsequent image processing will greatly increase execution time.

The CS algorithm provides a very robust processing pipeline in comparison to the FBP, offering the ability to select the important details within the image, and the acceptable amount of error in the name of increasing performance. It is also less susceptible to poor scans, using several sparsifying transforms to massively clean up the image output. The

biggest disadvantage is the performance, with image quality coming at the expense of computation time.

Ultimately, the Filtered Backprojection approach will work well for a Proof of Concept iteration of the *VALIS* system. Providing a more polished image reconstruction via Computed Sensing will be an objective of the prototype product.

The listed design requirements for each stage of development reflect the analysis performed in this section.

Design ID	Design Specification
Des. 3.7.1-C	Program must run on a consumer-grade computer by minimizing computational complexity in design
Des. 3.7.2-C	Reconstruction will utilize MATLAB, MathWorks, and K-Wave toolboxes to simplify and optimize computation
Des. 3.7.3-C	Software will be able to display the raw scan data corresponding to the transducer rotation about the ROI
Des. 3.7.4-P	Program will display image corresponding to 10-100μm scan area with high quality via Computed Sensing implementation
Des. 3.7.5-P	Target image detail will be tunable by user defined transform weighting coefficients *in Computed Sensing
Des. 3.7.6-P	Program performance will be alterable by user defined error, establishing a direct correlation between performance and image quality
Des. 3.7.7-P	Program will display GUI where the user can define settings, perform actions and interact with the device. Useful settings may include screen capture, screen recording, and stream pause.

Table 3.7.2 Design requirements for the Image Processing and Reconstruction

4. Test Plan, Standards and Safety

4.1 Test Plan by Development Phase

The test plan for the proof of concept is listed in Appendix A, which focuses on meeting the requirements set for the proof of concept in this document. These requirements sufficiently show the basic functions of the system and display the physical phenomena that generates the images.

For the next phase of development, the testing will focus on the requirements listed for the prototype. This test plan will be carried out by imaging animal tissue to further investigate the imaging capabilities of the system. It will also test how the system interacts with tissue, and will offer insight into the depth of imaging, image resolution and the usability of the system. In addition to testing the imaging requirements, we can also test the sustainability of the system, including the ability to be disinfected between uses. This method of testing

is prevalent in many other Photoacoustic Imaging systems, and is demonstrated in a multi-scale PAT experiment that was performed on a mouse with a subcutaneously inoculated tumor, with a chicken breast overlaid on the tumour to demonstrate imaging depth [17], as shown in Figure 4.2.1.

Finally, for the last phase of development, we will test the requirements for the final product. These tests have a large focus on engineering standards, safety, and usability of the product. To meet these requirements, testing must be completed in vivo, through clinical trials. This testing stage must prove the safety, efficacy and use cases of the device and must be approved by the appropriate regulatory bodies i.e. FDA, IEC, CSA.

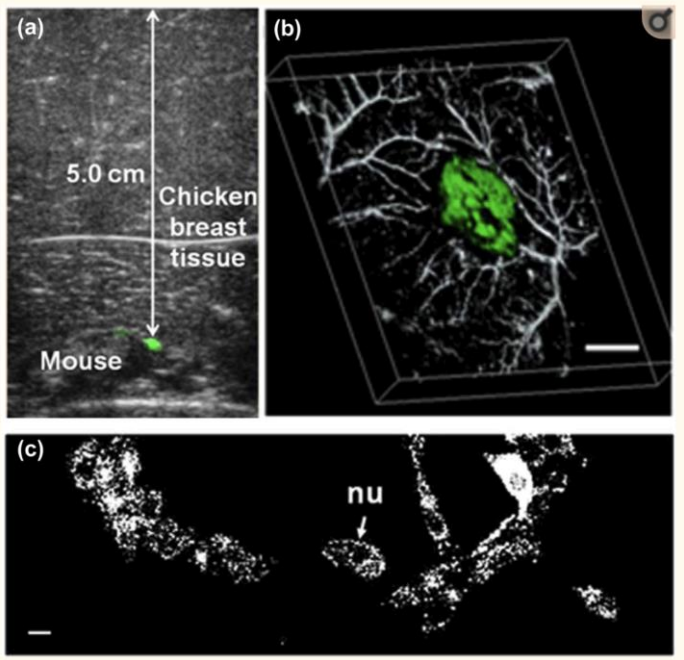

Figure 4.1.1: Multi-scale photoacoustic images of LacZ gene expression (a) B-scan image of a lacZ-marked tumor at a 5-cm depth in biological tissue, acquired by overlaying chicken breast tissue on top of a mouse. (b) 3D depiction of a composite photoacoustic image showing the tumor and blood vessels imaged with AR-PAM. (Green: tumor) (c) OR-PAM image of fixed lacZ cells grown on a cover glass after staining with Xgal. [17]

4.2 Device Safety

Optical safety is of the highest concern for PAI systems. Although we are implementing LEDs rather than a laser as the excitation source, many of the safety concerns and regulations are the same. Laser safety standards for in-vivo applications are defined by ANSI [29]. The standards are defined by the laser's optical wavelength, pulse duration, and exposure time. For example, at a wavelength of 500 nm and a pulse duration of 1 µs, the maximum permissible exposure (MPE) is 34.8 mJ/cm^2. This value is constant through to 700 nm wavelengths with the same pulse duration. Shown in figure 4.3.1. is a plot of the MPE versus wavelength for various pulse durations. We will ensure to stay below this threshold while developing our device.

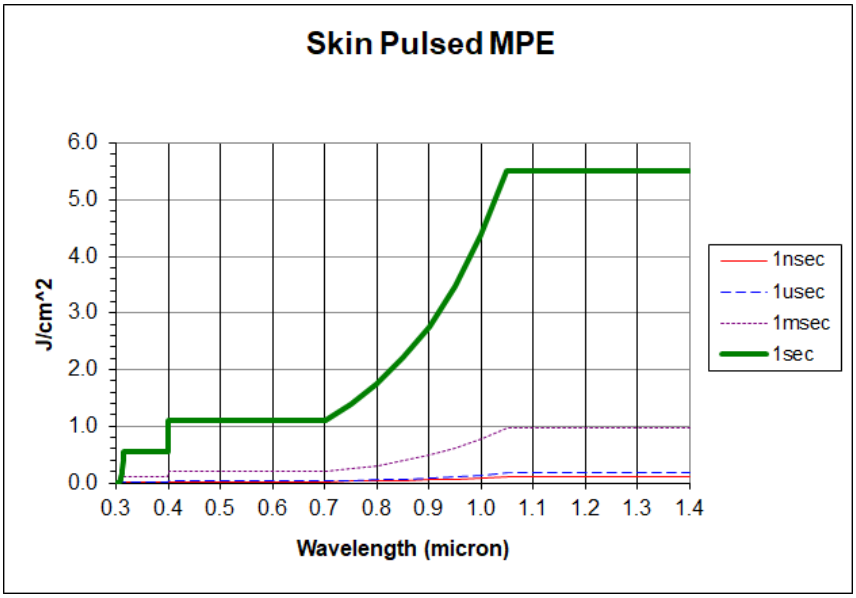

Figure 4.2.1: Skin MPE for a pulsed laser in the visual and IR region [30]

Our light source has a wavelength of 523 nm and has the same or very similar MPE values as most of the visible spectrum. Although the pulse duration is not definitively defined, the minimum power emitted in a pulse is expected to be 1 mJ. To increase both safety surrounding the EM source and the area being imaged, the light beam diverges from the emission source and covers a larger area. This in turn reduces the fluence, the power density of the light source.

When it comes to light sources, eyes are the part of the body that is most at risk. Ultraviolet and far IR light is absorbed by the cornea, while visible and NIR reaches the retina. The human eye has incredible focusing capabilities. For example, when a 1 mm laser beam is focused on the retina the power density can be increased by up to 62500 times. As safety is of the utmost concern, a power switch will be added to the handheld housing for the transducer and LEDs. Also, an IR proximity sensor will be included to ensure the LEDs will only turn on once the probe is close to the surface it will be imaging. This will significantly reduce the risk of the light being shined in anyone's eyes. Further details on the proximity sensor can be found in section 3.4. Figure 4.3.2, shown below, illustrates how light is focused in the eye.

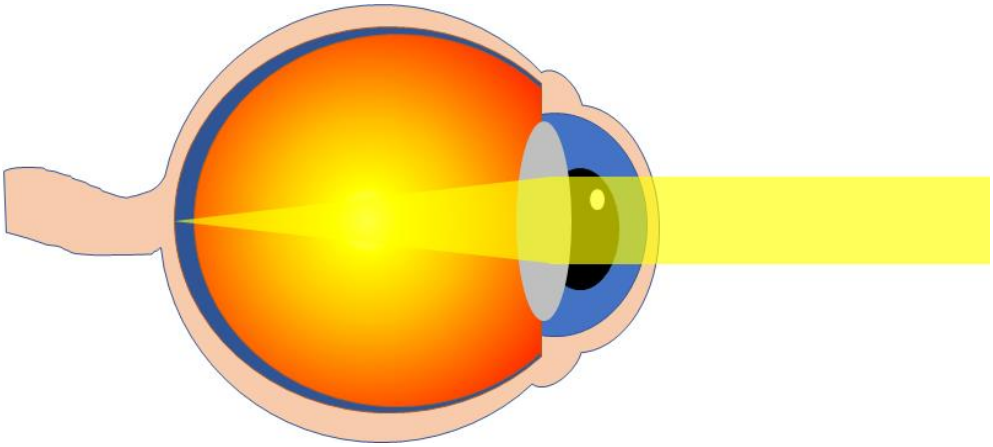

Figure 4.2.2: Light being focused in a human eye

The temperature of the device will be monitored to ensure it does not overheat. For temperature control, the LEDs will be pulsed, given them time to cool between each pulse, and heat sinks and possibly a fan will be added. Also, during use, if at any point there is a change in the functional state of the device, an alert will appear to inform the user of this change.

Various electrical safety precautions are being followed such as paths to ground to avoid oversupplying the electrical components or shocking the user or subject being imaged. The enclosure for the power supply will also be properly grounded. Detailed information on circuitry safety is included in section 3.4. Table 4.2.1 covers all the important design specifications regarding safety.

Design ID	Design Specification
Des. 4.2.1-P	The device will not exceed MPE ratings defined by the ANSI
Des. 4.2.2-C	This device will follow ANSI Z136 series of standards, outlining the safe use, testing and labeling of lasers [31]
Des. 4.2.3-F	This device will meet IEC 60601-1-9:2007 - collateral standard is to improve the environmental impact for the entire range of medical electrical equipment [32]
Des. 4.2.4-F	This device will be able to be easily disinfected for use on multiple patients
Des. 4.2.5-P	The handheld device and enclosure will not exceed leakage currents of over 10 mA to avoid macroshock to the patient [33]
Des. 4.2.6-C	The use and testing of light sources will abide by standards set out by WorkSafeBC OHS Part 7 [34]
Des. 4.2.7-C	The use and testing of lasers and light sources will abide by relevant standards set out by SFU for laser safety, oversight, training and exposure control [35]
Des 4.2.8-P	The LEDs will not turn on unless the device is within 1 cm of an object.
Des. 4.2.9-P	The electronic components will be protected by a grounded enclosure.

Table 4.2.1 Design requirements for device safety and sustainability

Conclusion

This document serves as a reference for the product design of VALIS's vascular photoacoustic imaging system. The subsystems required for this system include the light source with optical components, transducer array, DAQ with hardware control unit, and image acquisition and reconstruction software. Each product specification has been analyzed and chosen for our handheld application with the target market in mind.

The light source must have sufficient power per pulse and pulse frequency to generate measurable acoustic waves. The excitation light must also be at the absorption wavelength of hemoglobin. The light source must be focused by a lens to illuminate and focus the photons energy on only the region of interest.

The transducer will be implemented using a planar detection geometry for its versatility for our mobile hand-held array probe. A linear array transducer will be used for optimized image acquisition times. For our application of PAT, we plan to take advantage of existing, commercially available ultrasound scanners with a low-frequency range between 2-8 MHz.

The DAQ will be able to sample the various signals from the transducers in real-time, and send them to the imaging computer for further processing. It will also control the light source to fully synchronize the system. It will also employ safety precautions so that injury or damage is less likely to occur to users or patients, including several lockout devices.

The image reconstruction and processing program will be able to produce high-quality images with few noise artifacts using only MATLAB, Mathworks toolboxes, and a consumer-grade computer.

Test plans for the various development stages have been outlined, and the acceptance test procedures have been described in Appendix A for the proof of concept device. Relevant engineering standards to medical device safety, development, registration, testing, and high energy light source safety have also been listed, which the final product will have to abide by. Although these standards only apply to the final product, it is important to consider these standards at all steps of the development process.

Finally, the user interface and appearance specifications for the prototype design have been formalized in Appendix B. This document provides a detailed explanation of the products ease-of-use, appearance and software GUI.

References

[1] Medicalnewstoday.com. 2020. *CT Scan Or CAT Scan: How Does It Work?*. [online] Available at: https://www.medicalnewstoday.com/articles/153201#uses [Accessed 11 June 2020].

[2] Nibib.nih.gov. 2020. *Magnetic Resonance Imaging (MRI)*. [online] Available at: https://www.nibib.nih.gov/science-education/science-topics/magnetic-resonance-imaging-mri#:~:text=How%20does%20MRI%20work%3F,-MRI%20of%20a&text=MRIs%20employ%20powerful%20magnets%20which,pull%20of%20the%20magnetic%20field. [Accessed 11 June 2020].

[3] Mayoclinic.org. 2020. *Ultrasound - Mayo Clinic*. [online] Available at: https://www.mayoclinic.org/tests-procedures/ultrasound/about/pac-20395177#:~:text=There%20are%20no%20known%20risks,as%20the%20lungs%20or%20head [Accessed 12 June 2020].

[4] Jain, M., 2020. *Design And Development Of A Novel Photoacoustic Imaging System For Detection Of Intracranial Hemorrhages*. [online] Hdl.handle.net. Available at: <http://hdl.handle.net/11375/23811> [Accessed 11 June 2020].

[5] Wang, X., Chamberland, D. and Xi, G., 2008. Noninvasive reflection mode photoacoustic imaging through infant skull toward imaging of neonatal brains. *Journal of Neuroscience Methods*, 168(2), pp.412-421.

[6] Wang, Lihong V. *Photoacoustic Imaging and Spectroscopy*. CRC Press, 2017.

[7] Photoacoustics, vol. 14, no. January, pp. 1–11, 2019, doi: 10.1016/j.pacs.2019.01.004.

[8] P. Beard, “Biomedical photoacoustic imaging,” Interface Focus, vol. 1, no. 4, pp. 602–631, 2011, doi: 10.1098/rsfs.2011.0028.

[9] Y. Zhou, J. Yao, and L. V. Wang, “Tutorial on photoacoustic tomography,” *J. Biomed. Opt.*, vol. 21, no. 6, p. 061007, 2016, doi: 10.1117/1.jbo.21.6.061007.

[10] P. K. Upputuri and M. Pramanik, “Performance characterization of low-cost, high-speed, portable pulsed laser diode photoacoustic tomography (PLD-PAT) system,” Biomed. Opt. Express, vol. 6, no. 10, p. 4118, 2015, doi: 10.1364/boe.6.004118

[11] Mouser Electronics. 2020. *LZ4-00G108-0000 LED Engin | Mouser*. [online] Available at:https://www.mouser.ca/ProductDetail/LED-Engin/LZ4-00G108-0000?qs=aDBU8ng1tb%2F%252BiFLrPZUjww== [Accessed 12 July 2020].

[12] Mouser Electronics. 2020. *O-005S DBM Optix | Mouser*. [online] Available at: https://www.mouser.ca/ProductDetail/DBM-Optix/O-005s?qs=KObwnG1V4zuuL%252B15jdOizw%3D%3D [Accessed 12 July 2020].

[13] C. Sheaff and S. Ashkenazi, "Characterization of an improved polyimide-etalon all-optical transducer for high-resolution ultrasound imaging," in *IEEE Transactions on Ultrasonics, Ferroelectrics, and Frequency Control*, vol. 61, no. 7, pp. 1223-1232, July 2014, doi:10.1109/TUFFC.2014.3021.

[14] Yamashita Y., Hosono Y., Itsumi K. (2008) Low-Attenuation Acoustic Silicone Lens for Medical Ultrasonic Array Probes. In: Safari A., Akdoğan E.K. (eds) Piezoelectric and Acoustic Materials for Transducer Applications. Springer, Boston, MA

[15] Zhou, Q., Lam, K. H., Zheng, H., Qiu, W., & Shung, K. K. (2014). Piezoelectric single crystals for ultrasonic transducers in biomedical applications. *Progress in materials science*, *66*, 87–111. https://doi.org/10.1016/j.pmatsci.2014.06.001

[16] Choi, Hojong, et al. “Development of an Estimation Instrument of Acoustic Lens Properties for Medical Ultrasound Transducers.” *Journal of Healthcare Engineering*, vol. 2017, 2017, pp. 1–7., doi:10.1155/2017/6580217.

[17] Xia, J., Yao, J., & Wang, L. V. (2014). Photoacoustic tomography: principles and advances. *Electromagnetic waves (Cambridge, Mass.)*, *147*, 1–22. https://doi.org/10.2528/pier14032303

[18] Erfanzadeh, M., & Zhu, Q. (2019). Photoacoustic imaging with low-cost sources; A review. Retrieved June 14, 2020, from https://www.sciencedirect.com/science/article/pii/S2213597918300375

[19] Saunders, O, et al. “Ultrasound Transducer Self Heating: Development of 3-D Finite-Element Models.” *Journal of Physics: Conference Series*, vol. 1, 2004, pp. 72–77., doi:10.1088/1742-6596/1/1/017.

[20] “General Data about Burns.” *Burn Centre Care* , 2006, burncentrecare.co.uk/about_burned_skin.html#:~:text=A%20burn%20is%20damage%20to,(less%20than%20a%20second).

[21] Lunt, James. “Large-Scale Production, Properties and Commercial Applications of Polylactic Acid Polymers.” *Polymer Degradation and Stability*, vol. 59, no. 1-3, 1998, pp. 145–152., doi:10.1016/s0141-3910(97)00148-1.

[22] https://www.mathworks.com/help/images/radon-transform.html “Radon Transform.” *MATLAB & Simulink Help Center*, MATLAB & Simulink, www.mathworks.com/help/images/radon-transform.html.

[23] Peter Toft: "The Radon Transform - Theory and Implementation", Ph.D. thesis. Department of Mathematical Modelling, Technical University of Denmark, June 1996.

[24] “Iradon.” *MATLAB & Simulink Help Center*, MATLAB & Simulink, www.mathworks.com/help/images/ref/iradon.html#d120e177645.

[25] “CT Imaging.” *CISC 472, Lecture 3 - CT Imaging*, watkins.cs.queensu.ca/~jstewart/472/notes/02-ct/02-ct.html.

[26] Omidi, Parsa, et al. “A Novel Dictionary-Based Image Reconstruction for Photoacoustic Computed Tomography.” *Applied Sciences*, vol. 8, no. 9, 2018, p. 1570., doi:10.3390/app8091570.

[27] Simoncelli, Eero Peter., and Edward H. Adelson. *Subband Transforms*. Vision and Modeling Group, Media Laboratory, Massachusetts Institute of Technology, 1991.

[28] Selesnick, Ivan. “Total Variation Denoising (An MM Algorithm).” *OpenStax CNX*, cnx.org/contents/pQvNo0Ur@4/Total-Variation-Denoising-An-MM-Algorithm#:~:text=Introduction,terms%20of%20an%20optimization%20problem.

[29] L. I. of America, “American National Standard for Safe Use of Lasers,” Laser Inst. Am., 2007.

[30] Chapman, G., 2020. *Laser Safetytraining: Notes Downloads*. [online] Www2.ensc.sfu.ca. Available at: http://www2.ensc.sfu.ca/people/faculty/chapman/e894/lasersafety.html [Accessed 12 July 2020].

[31] “ANSI Z136 Standards,” *The Laser Institute*, 03-Oct-2018. [Online]. Available: https://www.lia.org/resources/laser-safety-information/laser-safety-standards/ansi-z136-standards. [Accessed: 14-Jun-2020].

[32] “IEC,” *IEC 60601-1-9:2007 | IEC Webstore*. [Online]. Available: https://webstore.iec.ch/publication/2601. [Accessed: 14-Jun-2020].

[33] C. F. Dalziel, “Electric shock hazard,” *IEEE Spectr.*, vol. 9, no. 2, pp. 41–50, 1972, doi: 10.1109/mspec.1972.5218692.

[34] “WorkSafe BC OHS Regulation Part 7: Noise, Vibration, Radiation and Temperature” [Online]. Available: https://www.worksafebc.com/en/law-policy/occupational-health-safety/searchable-ohs-regulation/ohs-regulation/part-07-noise-vibration-radiation-and-temperature. [Accessed: 14-Jun-2020].

[35] “SFU Safety and Risk Services: Laser Safety” [Online]. Available: https://www.sfu.ca/srs/work-research-safety/research-safety/laser-safety/compliance-oversight.html [Accessed : 14-Jun-2020].

[36] "International Organization for Standardization," March 2018. [Online]. Available: https://www.iso.org/standard/67720.html. [Accessed 11, July 2020].

[37] "International Organization for Standardization," November 2002. [Online]. Available: https://www.iso.org/standard/25578.html. [Accessed 11, July 2020].

[38] "International Organization for Standardization," September 2015. [Online]. Available: https://www.iso.org/standard/66767.html. [Accessed 11, July 2020].

[39] "International Organization for Standardization," March 2016. [Online]. Available: https://www.iso.org/standard/59752.html. [Accessed 11, July 2020].

[40] "IEC System of Conformity Assessment Schemes for Electrotechnical Equipment and Components," 18 February 2011. [Online]. Available: https://www.iecee.org/dyn/www/f?p=106:49:0::::FSP_STD_ID:5515. [Accessed 11 July 2020].

[41] "International Organization for Standardization," October 2010. [Online]. Available: https://www.iso.org/standard/44863.html. [Accessed 11, July 2020].

[42] "IEC System of Conformity Assessment Schemes for Electrotechnical Equipment and Components," 25 February 2011. [Online]. Available: https://www.iecee.org/dyn/www/f?p=106:49:0::::FSP_STD_ID:2667. [Accessed 11 July 2020].

[43] "IEEE Standards Association," 2017. [Online]. Available: https://standards.ieee.org/standard/2700-2017.html. [Accessed 15 June 2018].

[44] "International Organization for Standardization," February 2015. [Online]. Available: https://www.iso.org/standard/63179.html. [Accessed 11 July 2020].

[45] "International Organization for Standardization," March 2016. [Online]. Available: https://www.iso.org/standard/59752.html. [Accessed 11 July 2020].

[46] "International Organization for Standardization," March 2018. [Online]. Available: https://www.iso.org/standard/67720.html. [Accessed 11 July 2020].

[47] "IEC System of Conformity Assessment Schemes for Electrotechnical Equipment and Components," 15 May 2014. [Online]. Available: https://www.iecee.org/dyn/www/f?p=106:49:0::::FSP_STD_ID:3587. [Accessed 11 July 2020].

[48] "IEC System of Conformity Assessment Schemes for Electrotechnical Equipment and Components," 11 January 2011. [Online]. Available: https://www.iecee.org/dyn/www/f?p=106:49:0::::FSP_STD_ID:2676. [Accessed 11 July 2020].

Technical Appendices

A. Acceptance Test Procedures for Proof of Concept

In terms of functionality, the VALIS system is not expected to work flawlessly for the proof of concept; rather, the goal is to prove the validity of the PA theory. To this end, the following deliverables will be present for the PoC demo at the end of ENSC 405W:

- Light source + Optical system to excite tissue and generate acoustic waves
- Ultrasound transducer handheld probe to receive the acoustic waves
- Data acquisition circuitry to process the transducer signal
- Preliminary software implementation to record and display the output data

The culmination of these subsystems will be some presented image output corresponding to light source activation, thereby proving the generation of acoustic waves upon tissue excitation. Making sense of this output, and successfully reconstructing the image will be the goal for the prototype stage of development in ENSC 440. The acceptance test procedure entails fulfillment of the PoC requirements outlined in this document.

Tester name:		Date:	
Full System			
Relevant Specs	Procedure	Result	Comments
Des. 2.0.1-C to Des. 2.0.3-C	The system produces images of the subject's vasculature with a minimum resolution of 500 µm	☐ Pass ☐ Fail	
Light Source and Optics			
Relevant Specs	Procedure	Result	Comments
Des. 3.1.1-C	Measure the wavelength of the light source with a Spectrometer. The light source should have a peak wavelength of 523 nm, ± %10	☐ Pass ☐ Fail	
Des. 3.1.2-C	Use a laser power detector to measure the power of the light source, by shining the light directly into the detector. The light source energy should be between 1 mJ and 10 mJ per pulse	☐ Pass ☐ Fail	

Des. 3.1.3-C	Use a laser power detector to measure the power of the light source, by shining the light directly into the detector. Connect the output of the power detector to an oscilloscope to measure frequency. The light source has a pulse frequency between 1 KHz and 10 KHz	☐ Pass ☐ Fail	
Des. 3.1.4-C	Use a laser power detector to measure the power of the light source, by shining the light directly into the detector. Connect the output of the power detector to an oscilloscope to measure pulse length.The light source has pulse between 100 ns and 10 µs	☐ Pass ☐ Fail	
Des. 3.1.1-C to Des. 3.1.5-C	Perform an image test on a sample with hemoglobin in it, and view the image produced by the device to verify the excitation light is able to cause hemoglobin to generate measurable acoustic waves. In the event this test fails, ensure to test the transducer and DAQ as well to determine where the problem arises.	☐ Pass ☐ Fail	
Des. 3.4.3-C	Turn on the light source and hold close to a subject to be imaged. The excitation light should illuminate an area at least the size of the transducer.	☐ Pass ☐ Fail	
Des. 3.4.13-C	Turn on power to the light source. The light source should be successfully powered by the power source.	☐ Pass ☐ Fail	
Transducer			
Relevant Specs	Procedure	Result	Comments
Des. 3.3.1-C	Turn on the device, and begin imaging a subject. View the image produced.Transducer array should be able to detect acoustic waves created by vibration of cells due to incident	☐ Pass ☐ Fail	

	light source If this test fails, ensure to test the light source and DAQ to determine where the problem lies.		
Des. 3.3.1-C	Turn on the device and begin imaging the subject. View input to DAQ from transducer on terminal. Transducer can successfully transmit voltage to DAQ unit	☐ Pass ☐ Fail	
DAQ			
Relevant Specs	Procedure	Result	Comments
Des. 3.3.1-C	Turn on DAQ components and connect to a computer, feed input of 5 V. DAQ is able to convert analog transducer signal to a digital signal for processing	☐ Pass ☐ Fail	
Des. 3.3.7-C	Turn on the microcontroller and connect to the computer. Execute a ping and echo to verify connection. Microcontroller is able to communicate with imaging software computer	☐ Pass ☐ Fail	
Des. 3.3.11-C	Turn on the microcontroller and verify available storage. Store values for as many elements as the transducer array. Microcontroller has enough memory to store as many samples as elements in the transducer array.	☐ Pass ☐ Fail	
Des. 3.3.4-P to Des 3.3.5 -C	Turn on the microcontroller and input a known signal at an expected frequency of the ultrasonic waves. The signal should be recreated without significant loss of data.	☐ Pass ☐ Fail	
Des 3.3.11-P	Input sample readings that exceed the temperature or current thresholds. The system should shut down all relevant hardware as a safety precaution	☐ Pass ☐ Fail	
Image Reconstruction			
Relevant Specs	Procedure	Result	
Des. 3.7.1-C	Open program on consumer grade program and run. Program	☐ Pass	

	must run on a consumer-grade computer	☐ Fail	
Des. 3.7.2-C	Reconstruction will utilize MATLAB, MathWorks toolboxes and begin after initial power up and startup. Was the reconstruction successful?	☐ Pass ☐ Fail	
Des. 3.7.3-C	Upload raw data sets of scan data, and run the program with the data as input. Software will be able to display raw scan data	☐ Pass ☐ Fail	
Safety and Sustainability			
Relevant Specs	Procedure	Result	Comments
Des. 4.2.2-C	This device follows ANSI Z136 series of standards.	☐ Pass ☐ Fail	
Des. 4.2.6-C	The use and testing of lasers abides by standards set out by WorkSafeBC OHS Part 7	☐ Pass ☐ Fail	
Des. 4.2.7-C	The use and testing of lasers abides by standards set out by SFU for laser safety, oversight, training and exposure control	☐ Pass ☐ Fail	
Other			
Relevant Specs	Procedure	Result	Comments
Des. 3.4.9-C	Turn on the power supply to LEDs. Using appropriate current measuring devices such as Digital Multimeter, measure the current through the LEDs. The current should not exceed 1.5 A.	☐ Pass ☐ Fail	
Des. 3.4.9-C to Des. 3.4.10-C	Turn on the power supply. Measure the voltage from the power supply by using a DMM and connection probe to input pin and ground. The voltage across a LED should not exceed 16.8 V and the maximum current from the power supply should not exceed 16 A.	☐ Pass ☐ Fail	
Des. 3.4.11-C	Connect transistors used for switching light source to a microcontroller . Connect the output to an oscilloscope and	☐ Pass ☐ Fail	

	pulse the transistor at 1 to 10 kHz. View the output on the oscilloscope, calculate rise and fall time of the transistor and ensure they are less than 10 ns each.		
Des. 3.5.1-C	Isolate the two stage voltage amplifiers. Input 1 V to circuit, and measure output voltage. The output voltage should be larger than 40 db the input voltage.	☐ Pass ☐ Fail	
Des. 3.5.2-C	Isolate the two stage amplifier circuit. Input 1 V signal with frequency components with a bandwidth larger than transducer bandwidth. View the output on an oscilloscope, and ensure the bandwidth is the same as the transducers. The signal should attenuate outside of the transducer's bandwidth	☐ Pass ☐ Fail	
Des. 3.5.3-C	Isolate the two stage amplifier circuit. Feed the input some voltage and measure the outputted voltage after the diode. The voltage should be above or equal to zero.	☐ Pass ☐ Fail	
Des. 3.5.4-C	Feed the two stage amplifier circuit an input with frequency of 10 MHz. View the output and ensure the output has the proper characteristics and the op amps are correctly operating.	☐ Pass ☐ Fail	

B. UI / Appearance-Prototype Design Appendix

B.1 Introduction

This document aims to provide the users the training and understanding required to operate VALIS effectively and safely. The different settings and features will be outlined. Since VALIS is a non-invasive medical imaging device, we aim to provide patients and users with complete comfort, ensure safety, and provide an inexpensive alternative imaging method all while not compromising image quality. Our product will run on familiar software and be visually displayed in a completely intuitive manner. Additionally, the document will highlight the various design considerations including the user analysis, technical analysis and the engineering standards. The document will also include analytical usability testing undertaken by designers and a complete empirical usability testing for users.

VALIS was designed to be as user friendly as possible, requiring only a button on the power supply module and on the handheld imaging device to begin the imaging process. On the interactive screen, various features are implemented with intuitive symbols for ease of use. Furthermore, straightforward instructions are given upon startup and available whenever needed to minimize time required to learn how to operate VALIS.

B.2 Purpose

The purpose of the UI/Appearance appendix is to provide both a detailed explanation of the user interface of VALIS as well as the physical appearance of the device in both the proof of concept and the prototype phases. We will prove explanations for our design decisions and explain how each decision had the end user in mind.

B.3 User Analysis

VALIS, being a medical device, is mainly targeted towards physicians, patients, and researchers. The surging rate in non-transmissible diseases, such as stroke and cancer, drives the market growth of medical devices such as VALIS across the globe. As VALIS' main objective is to be an affordable and versatile real time imaging system, the design was taken into consideration with the assumption that the user has access to some hardware components and software required.

To power the device and obtain the necessary data for image reconstruction, a computer with MATLAB will be required. The system will require a connection to the computer via a USB in order to have the data collected and projected into an image. With those requirements, the user for VALIS is expected to have some prior experience with running MATLAB scripts for the backprojection needed to construct the image. To eliminate any confusion, a detailed guide with images will be provided to demonstrate a user-friendly step-by-step guide on how to connect the device, use the device, and run the MATLAB script to obtain their desired image.

In addition to the hardware and software requirements, VALIS does not use a tunable light source for imaging. The wavelength for the device has been set specifically for imaging the vasculature. This fact will be clearly labelled in both the packaging and the instructions

manual to notify the users of the limitation. With those clearly labelled, the users are expected to know the use case for VALIS before purchasing the device.

VALIS will consist of a handheld probe that is connected via wired communication and power line to the power supply, microcontroller and other hardware components. The operator will be required to, with high dexterity, orient the probe on the surface of the patient or phantom being imaged.

Due to the hardware and software requirements as well as the restricted wavelength application of the system, the main target for VALIS will be researchers that have the necessary background knowledge and the hardware and software components.

B.4 Graphical Presentation

Figure B.4.1 shows a graphical representation of the hand help probe that will be used for both illuminating the tissue being imaged as well as receiving the acoustic waves that result. The probe is designed to be both comfortable to hold, lightweight and of familiar size. The connecting communication and power wire bundle will enter the probe at the rear, and continues beyond the figure to the data acquisition unit and power supply. The transducer has been designed to protrude beyond the surface of the LEDs to ensure complete contact with the tissue being imaged while also protecting against direct contact with the LED lenses which may become slightly hot.

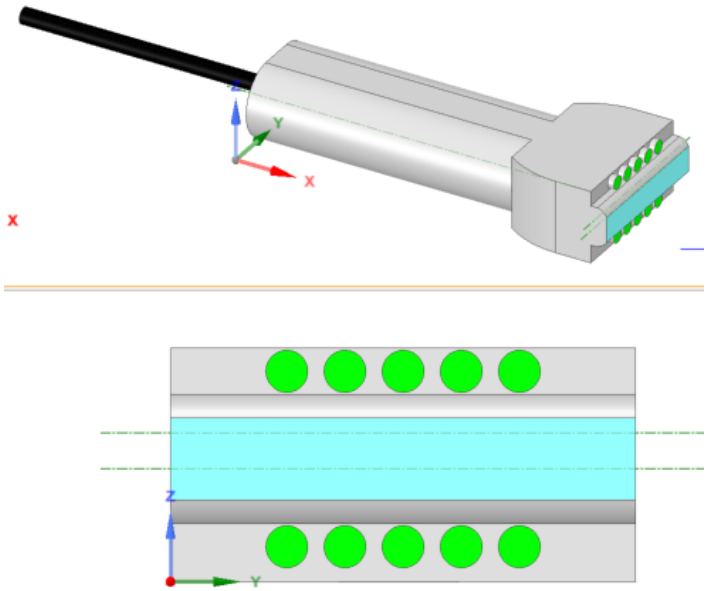

Figure B.4.1: A 3D CAD model of the handheld probe, with connecting communication wire (black), Light sources (green) and transducer array (light blue)

Below in Figure B.4.2 we see some sample frames from the proposed prototype GUI. The GUI has the image displayed front and center, and clearly defines the depth of the various parts of the image. Along with this information, more information such as study name, series name, image name and the date and time are visible. Details concerning the imaging settings are also listed on the left of the screen, displaying the transducer frequency, gain, frame rate, contrast and depth of imaging. Finally icons representing different features are displayed in the bottom left corner, with icons to power off the device, record images being

acquired, take a screen capture of the current frame, freeze on the current frame, manage settings and finally open info dialogue. The welcome screen will show when the device is first powered on, and will explain the features and how to begin imaging. This menu will also be available when selecting the info icon.

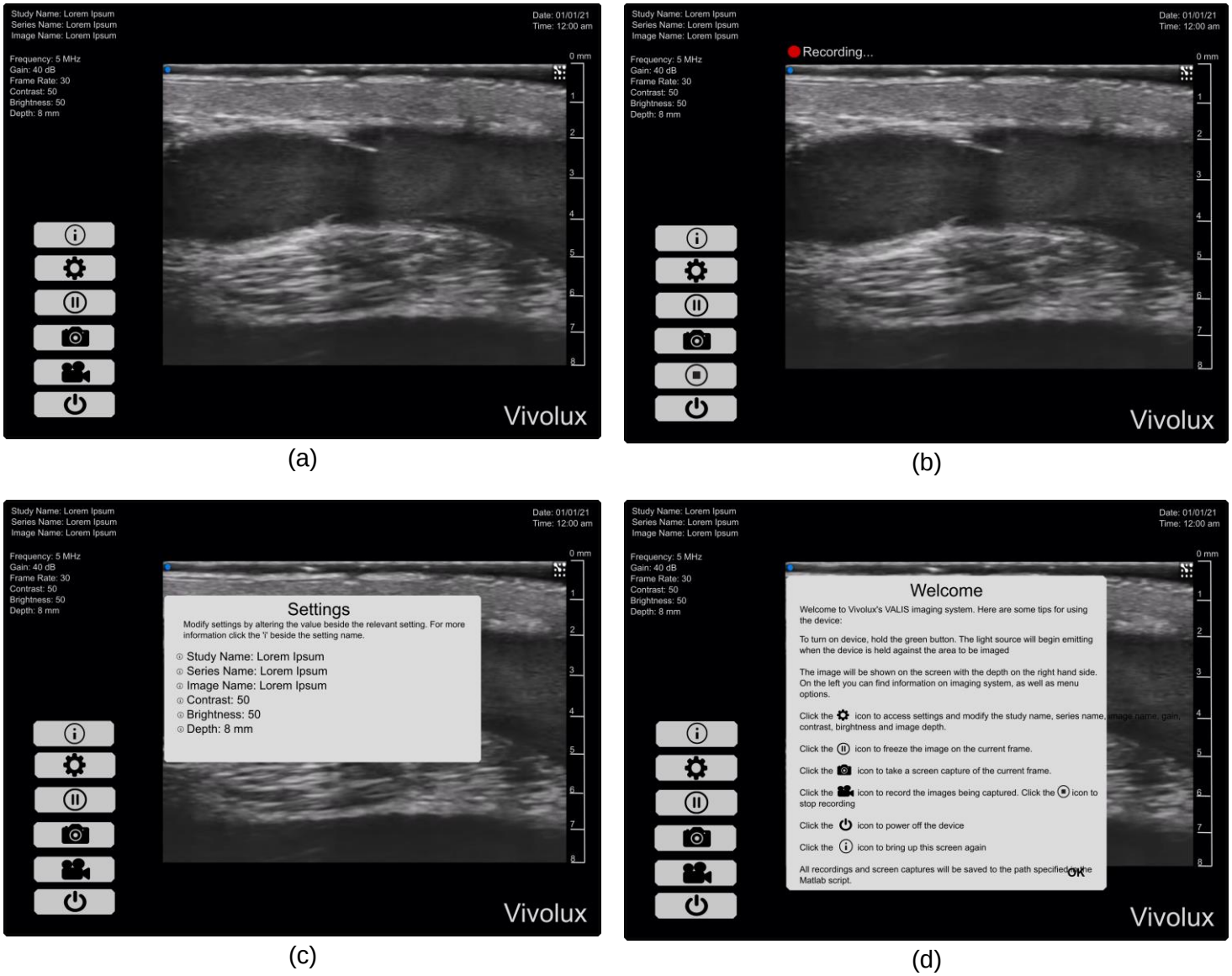

Figure B.4.2: (a) Example GUI for the general use of the device (b) Screen showing the recording process of the images being collected (c) Settings menu outlining the different options (d) Welcome message that explains the basic use of the device and different features

B.5 Technical Analysis

From the text “The Design of Everyday Things” written by Don Norman, there are seven important considerations in design. The “Seven Elements of UI Interaction” (discoverability, feedback, conceptual models, affordances, signifiers, mappings, constraints) have been taken into consideration in the following ways.

Discoverability refers to the familiarity of the device when being used for the first time. In a sense, how similar it is to other well known products in the way it behaves, feels and displays. With our prototype for VALIS we have a number of key design implementations that aim to make the device both comfortable and user-friendly.

1. The hand-held probe will have roughly the same lateral dimensions to that of a smartphone. This is to match the familiarity of a device that a user would handle daily in terms of both dimensions and weight.
2. The device software will run as a simple MATLAB script. As our product will be primarily sold to researchers, running a simple script in MATLAB will be familiar.
3. Our prototype will be designed to have a button signifying the on/off switch built onto the probe and located near the index finger.
4. The DAQ/LED controller module will have a red switch that will control the power to the entire unit, including a label as well as direction indication of on or off.
5. The GUI will contain familiar icons such as a camera indicating the control for screen capture, a video camera indicating the control for screen record and a pause icon that controls a screen pause.

Feedback refers to the device responding in some manner to a user's action using the device. Our prototype will implement a number of simple feedback systems as follows:

1. The power control switch will have a small green LED directly beside the switch indicating that the unit has been powered on
2. When running the provided MATLAB script, a GUI will be displayed immediately
3. When imaging is ready to begin the the MATLAB GUI will clearly display a message prompting the user to begin
4. The prototype will display an image in real-time as the user being to probe the patient or phantom being studied
5. Any warning indicators will be displayed directly over the image to indicate a change in functional state and alert the user

Conceptual Models refers to the image of how the device functions that the user develops in their mind as developed from previously used items and their general life experiences. With VALIS, the user experience will be nearly identical to that of an ultrasound probe. As the PAI system is intended primarily for researchers, most will be fully familiar with the process of running ultrasound. In addition the already user-friendly interface of MATLAB keeps the software easy to navigate.

Affordance refers to the object's properties and how those properties suggest to the user how and what it can be used for. Our VALIS prototype consists physically of an ergonomically designed handheld probe which will shape the hand in such a way that it will be comfortably held in the proper orientation for imaging. The single button on the probe which allows for image acquisition ensures that the user will not have hesitations on its function. The user facing GUI will have clear menu options as well as familiar icons that direct the user towards the functions they want.

Signifiers refer to the indicators of the possible affordances of the device. Our prototype of VALIS will employ a number of signifiers. The power switch located on the control unit will

have clear labels indicating on or off. The GUI will display a message when it is ready to image with brief instructions on how to begin imaging. The real-time image displayed will also be a signifier of what the system is capturing. If there is a change in functional state, warning indicators will appear on the screen to alert the user.

Mapping refers to how two components of a design are shown to interact with each other to the user. Since VALIS has a minimalist design in terms of varying function, it only has two major operation components. The power button, which will be clearly labelled for on and off, and the image acquisition button located on the handheld probe. The button, when suppressed will allow an image to be displayed on the screen giving a clear map to its function.

Constraints refers to the limitations on how the design can be used and what it is not capable of being used for. There are a number of constraints for the prototype of VALIS:

1. The user must own a moderate to high end PC with sizable ram (minimum 8 GB), a decent processor (recommended specification: i5 5th generation - Broadwell or above).
2. The user must have access to a MATLAB license and be able to run a provided script
3. The user must have a display monitor that is interfaced with the PC
4. The PC must have a USB port to interface with the DAQ
5. The user is required to have access to a 120 V outlet to power the device
6. The user is required to operate the handheld probe with the same level of dexterity required in sonography
7. The device is designed specifically to image vascular either in-vivo or on a phantom
8. The device will come with set parameter that indicate maximum penetration depth and resolution achievable under a standard set of parameters

B.6 Engineering Standards

Throughout development of the Photoacoustic Imaging system, the relevant engineering and medical device standards must be considered, to streamline any clinical trials and device approval. Although the standards will only apply to the final product, it is worth designing the prototype to meet these standards as well.

Some important standards collections for biomaterials and biomedical engineering include:

- IEC - International Electrotechnical Commission
- IEEE - Institute of Electrical and Electronics Engineers
- ISO - International Standard Organization

VALIS will be designed to meet the engineering standards from organizations such as the ISO, IEC and IEEE displayed in Table B.6.1 below.

Standard ID	Description of Engineering Standard
ISO 14915-1	Standards for visual user-interface elements presented by software [36]

ISO 80002	Standard for validation of medical device software quality systems [37]
ISO 13485:2016	Standard for medical devices - quality management systems [38]
ISO 14199:2015	Standard Information models - Biomedical Research Integrated Domain Group (BRIDG) [39]
IEC 61508-1:2010	Standard for functional safety of electronic safety-related systems [40]
ISO 80001-1:2010	Standard for risk management of safety, effectiveness, and security in the implementation and use of connected medical devices or health software [41]
IEC 60601-2-49	Medical electrical equipment standard – requirements for the basic safety and essential performance of multifunction patient monitoring equipment [42]
IEEE 2700-2017	Standard for Sensor Performance Parameter [43]
IEC 62366-1:2015	Standard of Medical devices -- Application of usability engineering to medical devices [44]
ISO 13485:2016	Standard of Medical devices -- Quality management systems -- Requirements for regulatory purposes [45]
IEC 80601-2-49:2018	Standard for medical electrical equipment: Particular requirements for the basic safety and essential performance of multifunction patient monitoring equipment [46]
IEC 60825-1:2014	Standard for laser products - Equipment classification and requirements [47]
IEC 60601-2-57:2011	Standard for medical electrical equipment - Particular requirements for the basic safety and essential performance of non-laser light source equipment [48]

Table B.6.1 Engineering standards relevant to the design and operation of *VALIS*

B.7 Usability Testing

Usability testing is performed to gain detailed insight on performance, safety and common difficulties users may face when interacting with the device. This usability testing will outline both analytical and empirical usability testing procedures to navigate the users for troubleshooting their respective problems. These tests are intended to reduce usage risk

and result in cost savings by reducing development time and liability. Careful planning will be essential and the testing will be conducted by an unbiased user that has the prerequisite knowledge highlighted in the market and will be frequently updated as the progress on the project continues.

B.7.1 Analytical Usability Testing

The analytical usability testing will highlight general usability questions the consumer may have. The usability testing will be divided into general usages and the main components.

General Usage

- The probe in contact with the patient is in appropriate thermal range to prevent damage to the skin
- Remove any imperfections on the probe before using to ensure no contamination is blocking the light source or the transducer

Light source / LED

- Light source needs to be correctly connected to the power supply ensuring both the on/off switches are on and powered with the right supply voltage and current
- Check alignment of the conical lens for each LEDs for the excitation beam in order for them to correctly concentrate on the region of interest

Transducer

- Keep in planar geometry for accurate data collection
- Ultrasound gels (commonly composed of water and propylene glycol) can be used to reduce acoustic attenuation and impedance

Data acquisition / Image reconstruction

- Quality of data acquisition and image reconstruction is largely dependent on the quality of the scan
- Large error tolerance will yield better temporal performance but worse reconstruction. Conversely, small error tolerance will sacrifice speed for image quality

B.7.2 Empirical Usability Testing

The empirical usability testing is an important component when verifying the devices usability. In many cases, certain aspects of a device may be inefficient, but it is hard to analytically explain these shortcomings. In this case, it is important to also consider qualitative observations as well, and design the device to be usable according to analytic standards, but also empirical ones. Below are some empirical questions consumers may have concerning the use of the device, at different stages of development. It is important to note that given the experimental nature of the device, ease of use is not anticipated at the Proof of Concept stage of development; the device shall nevertheless exhibit behaviour and results indicative of component functionality.

Proof of Concept:

General Usage

- Errors are explained and correctable

Light source / LED

- Light source malfunctions can be diagnosed fixed with minimal effort

Transducer

- Transducer can effectively transmit data to DAQ
- Transducer can effectively collect data from acoustic waves

Data acquisition / Image reconstruction

- The DAQ can relay data to the processing computer corresponding to the transducer scan
- The processing computer will be able produce tangible output corresponding to transducer scan data

Prototype:

General Usage

- The device is easy and intuitive to power on
- The Matlab script is straightforward and the GUI is easy to use
- The power cord and any other connections are long enough for the device to be mobile, but not too long they become cumbersome
- The device is able to be easily transported and stored
- Error messages are clear and easy to understand
- Errors are easy to correct and recover from

Light Source/LED

- The light source is sufficiently isolated from the user
- The proximity sensor prevents accidental exposure
- The light source does not hurt, itch, or burn the subject when imaging

Transducer

- The temperature of the enclosure is cool enough to handle
- The transducer can be easily maneuvered in order to get the ideal viewing angle
- The transducer is light enough to be handled for long periods of time

Data acquisition / Image reconstruction

- The image quality is sufficient for purpose
- The image is displayed quickly and correctly
- The image settings are intuitive to use
- The DAQ is easy to connect to a computer

B.8 Conclusion

The ease of use for any device is one of the most important aspects when designing a well-made product. Our product was designed with familiar software and intuitive GUI to ease interaction with the device. The UI appendix was designed to provide the users with the necessary training and understanding required to operate VALIS effectively and safely. The user analysis, technical analysis and engineering standards were highlighted in order to provide further understanding of the device overall. Further testing methods will be conducted after the prototype design to improve usability with the feedback received to improve both analytical and empirical usability. For the proof of concept design, we aim to provide a minimalistic hand-held probe design that demonstrates data collection from the acoustic signals collected by the transducer. For the prototype design, we aim to meet our goals of having an easy to use, inexpensive method of accurately imaging the vasculature.